

แอมเพอโรเมตริกกลูโคสเซนเซอร์โดยใช้ขั้วไฟฟ้าทองคำเคลือบด้วยเฮกซะแอมมีนรูทีเนียม (III)  
คลอไรด์-เนฟิออน สำหรับการวิเคราะห์ฟลูออโรอินเจคชัน



นายภัสสรพล งามอุโฆษ

สถาบันวิทยบริการ

วิทยานิพนธ์นี้เป็นส่วนหนึ่งของการศึกษาตามหลักสูตรปริญญาวิทยาศาสตรมหาบัณฑิต

สาขาวิชาเคมี ภาควิชาเคมี

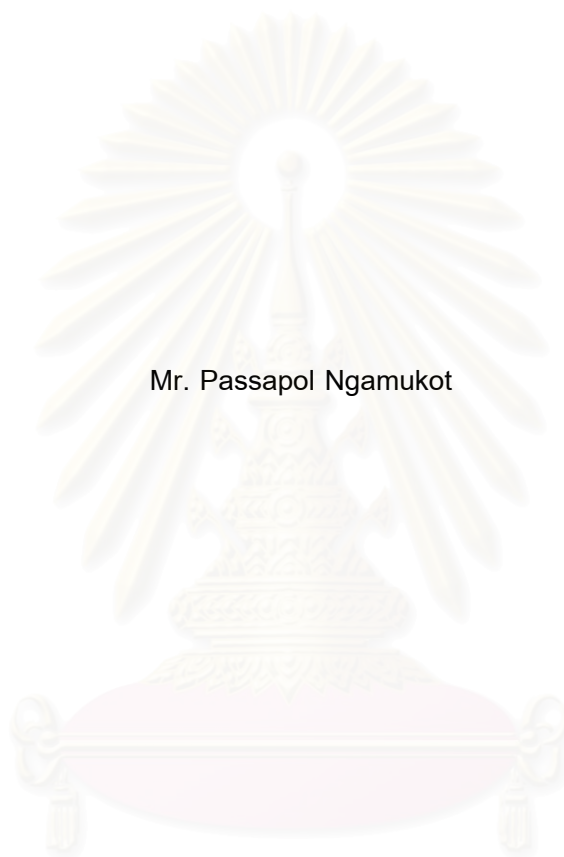
คณะวิทยาศาสตร์ จุฬาลงกรณ์มหาวิทยาลัย

ปีการศึกษา 2543

ISBN 974-13-1178-8

ลิขสิทธิ์ของจุฬาลงกรณ์มหาวิทยาลัย

AMPEROMETRIC GLUCOSE SENSOR USING  
HEXAAMMINERUTHENIUM (III) CHLORIDE – NAFION COATED  
GOLD ELECTRODE FOR FLOW INJECTION ANALYSIS



Mr. Passapol Ngamukot

A Thesis Submitted in Partial Fulfillment of the Requirements  
for the Degree of Master of Science in Chemistry

Department of Chemistry

Faculty of Science

Chulalongkorn University

Academic Year 2000

ISBN 974-13-1178-8



ภัทสรพีล งามอุโฆษ : แอมเพอโรเมตริกกลูโคสเซนเซอร์โดยใช้ขั้วไฟฟ้าทองคำเคลือบด้วยเฮกซะแอมมินรูทีเนียม (III) คลอไรด์-เนฟลอน สำหรับการวิเคราะห์โพลีอินเจคชัน (AMPEROMETRIC GLUCOSE SENSOR USING HEXAAMMINERUTHENIUM (III) CHLORIDE – NAFION COATED GOLD ELECTRODE FOR FLOW INJECTION ANALYSIS) อาจารย์ที่ปรึกษา : ดร. อรวรรณ ชัยลภากุล, 73 หน้า ISBN 974-13-1178-8

งานวิจัยนี้ศึกษาเกี่ยวกับวิธีการเตรียมแอมเพอโรเมตริกกลูโคสเซนเซอร์แบบใหม่ โดยการตรึงเอนไซม์กลูโคสออกซิเดสไว้ในฟิล์มของพอลิไพโรลซึ่งเตรียมด้วยวิธีพอลิเมอไรเซชันแบบใช้ไฟฟ้า โดยใช้ขั้วไฟฟ้าทองคำที่เคลือบด้วยเฮกซะแอมมินรูทีเนียม (III) คลอไรด์-เนฟลอน เฮกซะแอมมินรูทีเนียม (III) คลอไรด์ซึ่งทำหน้าที่เป็นตัวส่งผ่านอิเล็กตรอนยึดติดกับเนฟลอนโดยอาศัยแรงดึงดูดระหว่าง  $[Ru(NH_3)_6]^{3+}$  กับหมู่ซัลโฟเนตของเนฟลอนซึ่งมีประจุตรงข้ามกัน การตรวจวัดปริมาณน้ำตาลกลูโคสสามารถทำได้โดยใช้วิธีวิเคราะห์แบบโพลีอินเจคชัน และทำการบันทึกสัญญาณตอบสนองของน้ำตาลกลูโคสโดยใช้แอมเพอโรเมทรี ในงานวิจัยนี้ได้ทำการศึกษาสภาวะที่เหมาะสมในการเตรียมกลูโคสเซนเซอร์ รูปแบบของโพลีเมอร์ที่เหมาะสมและประสิทธิภาพของกลูโคสเซนเซอร์ที่เตรียมขึ้น จากการทดลองพบว่ากลูโคสเซนเซอร์ที่เตรียมได้สามารถวัดน้ำตาลกลูโคสได้ที่มีความเข้มข้นต่ำสุด 5 mM มีสภาพไวเท่ากับ 1.47 nA/mM เวลาที่ใช้ตอบสนองอยู่ในช่วง 25-50 วินาที สามารถใช้วิเคราะห์ได้อย่างน้อย 12 ครั้ง

สถาบันวิทยบริการ  
จุฬาลงกรณ์มหาวิทยาลัย

ภาควิชา.....เคมี.....  
สาขาวิชา.....เคมี.....  
ปีการศึกษา.....2543.....

ลายมือชื่อนิสิต.....  
ลายมือชื่ออาจารย์ที่ปรึกษา.....  
ลายมือชื่ออาจารย์ที่ปรึกษาร่วม.....

# # 4172388623 : MAJOR CHEMISTRY

KEYWORDS: AMPEROMETRIC GLUCOSE SENSOR / FLOW INJECTION ANALYSIS  
/HEXAAMMINERUTHENIUM (III) CHLORIDE PASSAPOL NGAMUKOT:  
AMPEROMETRIC GLUCOSE SENSOR USING HEXAAMMINERUTHENIUM  
(III) CHLORIDE – NAFION COATED GOLD ELECTRODE FOR FLOW  
INJECTION ANALYSIS THESIS ADVISOR: ORAWON CHAILAPAKUL,  
Ph.D. 73 pp. ISBN 974-13-1178-8

In this study, new preparation procedures of amperometric glucose sensor were investigated. The enzyme glucose oxidase was immobilized on the surface of hexaamineruthenium (III) chloride-Nafion coated gold electrode by entrapment in electropolymerized pyrrole film.  $\text{Ru}(\text{NH}_3)_6\text{Cl}_3$ , serve as electron mediator, was immobilized by the electrostatic interaction between  $[\text{Ru}(\text{NH}_3)_6]^{3+}$  and sulfonate groups of Nafion. The glucose determinations were performed using flow injection system. Glucose responses were determined by amperometry . With these glucose sensor, it was found that a detection limit was 5 mM and sensitivity was 1.47 nA/mM. The response time was 25-50 seconds. The operational stability of the glucose sensor was at least 12 times.



Department.....Chemistry.....

Field of study...Chemistry.....

Academic year.....2000.....

Student's signature.....

Advisor's signature.....

Co-advisor's signature.....

## ACKNOWLEDGEMENT

I would like to affectionately give all gratitude to my parents and family members for their wholehearted understanding, encouragement, and patient support throughout my entire study.

Gratefully thanks to Associate Professor Dr. Siri Varothai, Assistant Professor Kanyarat Kalampakorn and Dr. Sanong Ekgasit for their substantial advice as thesis committee.

I also would like to acknowledge Associate Professor Dr. Umaporn Titapiwatanakun for her useful suggestion about the flow injection system.

Finally, this thesis would never be successfully complete without the excellent advice from my thesis advisor, Dr. Orawon Chailapakul, who always provides me the useful guidance, suggestion, encouragement, and understanding during the whole course of research.

Passapol Ngamukot

สถาบันวิทยบริการ  
จุฬาลงกรณ์มหาวิทยาลัย

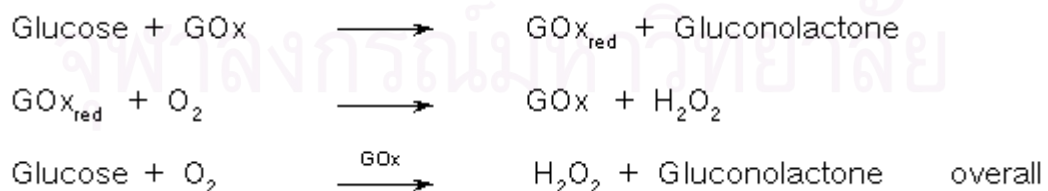
## CHAPTER I

### INTRODUCTION

#### 1.1 Problem Definition

Recently, electrochemical detection has clearly proved to be the favored method for use in biosensors. Electrochemical sensors can be divided into two categories: potentiometric devices that monitor the potential changes and amperometric devices that record the current flows when the potential is held at a constant value (1). The first category includes pH meters, ion-selective electrodes and ion-selective field effect transistors. These instruments suffer from the inherent characteristics of potentiometry, i.e., rather slow response to solutions at low concentrations of analyte and high detection limits. Amperometric determination offers better sensitivity, lower detection limits and relatively low cost.

A further classification of amperometric biosensors may be made into direct and indirect electron transfer systems (as shown in Figure 1.1). For a direct amperometric biosensor, electron transfer occurs freely between the redox center of a catalytic protein and the electrode (2). A cyanometalate-modified electrode based on direct electron transfer has been reported (3). A more practical way is the use of electron mediators that shuttle electrons between the protein and the electrode. A mediator becomes important in attempts to eliminate oxygen depletion effects on signals of oxidoreductase sensors. Consider the following problem in the case of amperometric glucose sensors.



Glucose oxidase is a flavoprotein, which catalyzes the oxidation of glucose to gluconolactone. The natural electron mediator is oxygen, which is reduced to hydrogen peroxide. The operating potential for this sensor is +0.7 V (vs. Ag/AgCl). At this potential, ascorbic acid and uric acid are very important interferences. The linearity of the calibration curve is affected by the depletion of oxygen in the sample. This mediated approach is used to remove oxygen dependence from the sensor's function and avoid the interferences. Several mediators have been reported (4, 5).

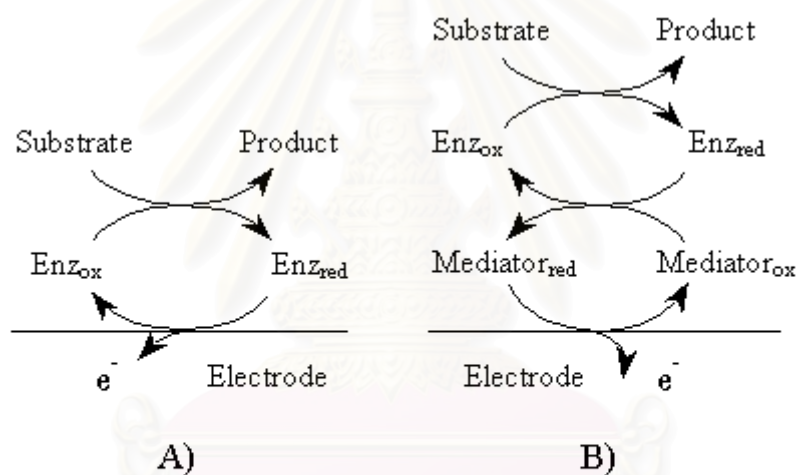


**Figure 1.1.** Schematic diagram of the direct electron transfer system (A) and the indirect electron transfer (B)

Compounds such as ferrocene have been shown to be well suited to this purpose. Systems with the application of conducting polymer-modified electrodes have been developed. The optimal conditions for the preparations of polypyrrole films on platinum electrodes have been reported (6, 7). The electropolymerization of polypyrrole, polythiophene and polyaniline on Nafion-modified electrode have been investigated (8).



## 1.2 Literature Review

Trojanowicz et al. used electropolymerized polypyrrole film to immobilize glucose oxidase on the surface of a platinum wire electrode (9). Glucose was determined using flow injection. An upper limit of linear response for an 100  $\mu\text{L}$  injected volume was estimated as 20 mM.

Tuner and co-workers used ruthenium (III) hexaammine as an electron mediator to fabricate a coulometric sensor for glucose based on thin-layer bulk electrolysis (10). The response was linear over the range 2-30 mM, which cover the normal accepted range for blood glucose level in diabetic patients.

Bartlett and Caruana immobilized glucose oxidase onto a platinum microelectrode by adsorption technique, followed by immobilization in an electrochemically polymerized phenol film (11). This process was found to be reproducible method for fabrication of enzyme electrodes. The electrodes were found to be stable for more than 40 days on storage at 4°C.

Van Os and co-workers fabricated a sensor by entrapping the enzyme glucose oxidase during polymerization of pyrrole onto a platinum electrode (12). The glucose responses were measured amperometrically at a potential of +0.7 V vs. SCE to detect hydrogen peroxide generated by the enzyme in the presence of oxygen. Flow injection was used for the glucose determination.

Pei and Li fabricated an amperometric glucose sensor by immobilizing glucose oxidase on a  $\text{CuPtCl}_6$  chemically modified electrode (13). The enzyme was immobilized via cross-linking of glutaraldehyde in the present of bovine serum albumin (BSA). The sensor provided a linear response to glucose over a concentration range of  $2 \times 10^{-6}$  to  $1 \times 10^{-3}$  M with a detection limit of  $1 \times 10^{-6}$  M.

Rivas and Rodriquez prepared a glucose biosensor by the deposition of iridium and glucose oxidase on a glassy carbon transducer (14). The electrocatalytic action of iridium towards hydrogen peroxide allows fast glucose quantification at low potentials.

The interference of easily oxidizable compounds such as ascorbic acid and uric acid is minimal.

Bartlett and co-workers used ferro/ferricyanide as the electron mediator for a glucose sensor (4). Glucose oxidase and ferro/ferricyanide were immobilized in an electropolymerized poly(*N*-methyl pyrrole) film. The two species compete for incorporation into the film so that on increasing the concentration of enzyme in the growth solution less ferro/ferricyanide is incorporated. The operating potential for glucose determination is 0.45V vs. SCE.

Atai and co-workers investigated the influence of polymerization conditions and film thickness on the activity and stability of the immobilized enzyme (15). Glucose oxidase was immobilized in thin polypyrrole films.

The amperometric glucose sensor using ferricyanide as the mediator has a high redox potential relative to compounds that may be present in a real sample, such as ascorbic acid and acetaminophen. These compounds may lead to a positive erroneous determination of glucose concentration. As the use of ferrocene is precluded by its low solubility and poor stability in the oxidized form, alternative mediators were sought. Hexaammineruthenium (III) chloride has an oxidation potential close to 0.0 V vs. SCE, therefore this complex was considered as a useful mediator.

### 1.3 Hypothesis

Ruthenium (III) hexaammine,  $[\text{Ru}(\text{NH}_3)_6]^{3+}$ , is capable of oxidizing reduced glucose oxidase in aqueous solution. The reduced form of the couple can also be reversibly oxidized by single electron transfer at a variety of solid electrodes with the half-wave potential ( $E_{1/2}$ ) equal to  $-215$  mV vs. SCE. The compatible features of  $[\text{Ru}(\text{NH}_3)_6]^{3+}$  for this work are: quasireversible electrochemistry at gold electrodes with a  $k^0$  equal to  $0.03$  cm/s, linear plots of  $I_p$  vs.  $v^{1/2}$  at constant concentration for the oxidation and reduction of the specie under diffusion control.

Because of its good solubility in aqueous media,  $[\text{Ru}(\text{NH}_3)_6]^{3+}$  has a high possibility of diffusion back in the bulk solution. This process may limit the sensor lifetime. Since  $[\text{Ru}(\text{NH}_3)_6]^{3+}$  is positively charged, the interaction between this specie and a negatively charged specie should be favorable. Polymeric pre-coating by a copolymer that contains negative charges is a new approach to prolong the stability of the sensors. In this research, perfluorosulfonate ionomers, trade name Nafion, was considered as a solution to the problem.

In this case,  $[\text{Ru}(\text{NH}_3)_6]^{3+}$  acts as a counterion for the sulfonate charges on the Nafion backbone. The interaction between these two species is called electrostatic binding (as shown in Figure 1.2).

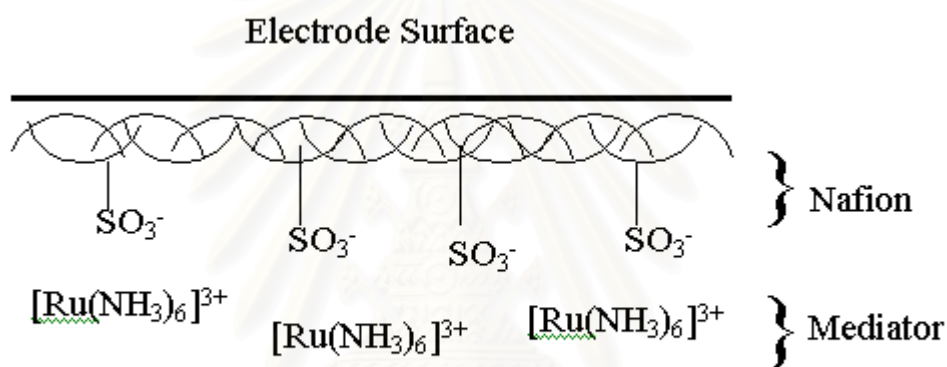


**Figure 1.2.** Schematic diagram of electrostatic binding

Glucose oxidase was immobilized by entrapping in an electropolymerized polypyrrole film. The operating potential for the determination of glucose can be reduced lower than 0.7 V.

สถาบันวิทยบริการ  
จุฬาลงกรณ์มหาวิทยาลัย

## 1.4 The Purpose of the Study

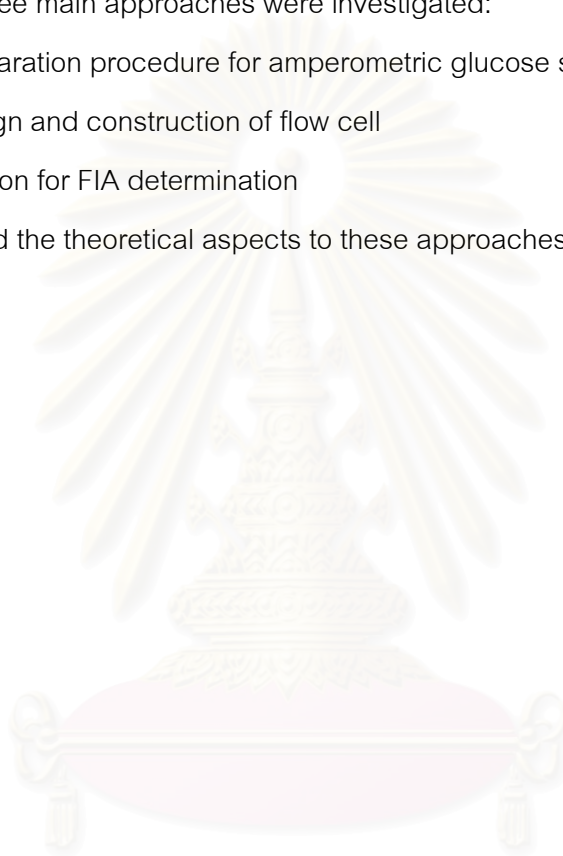
This work uses an amperometric glucose sensor as the detector in an FIA system for the determination of glucose. Glucose oxidase and  $\text{Ru}(\text{NH}_3)_6\text{Cl}_3$  were immobilized on a gold disk, pre-coated with Nafion, by entrapment in an electropolymerized film of pyrrole. An effective method with high sensitivity, selectivity, rapidity and reliability is the aim of this work. Three main approaches were investigated:

The new preparation procedure for amperometric glucose sensors

The new design and construction of flow cell

The optimization for FIA determination

The background and the theoretical aspects to these approaches are detailed in the next chapter.



สถาบันวิทยบริการ  
จุฬาลงกรณ์มหาวิทยาลัย

## CHAPTER II

### THEORY

#### 2.1 Bioanalytical Sensors

A bioanalytical sensor is an analytical device, incorporated with a biological-sensing element, providing quantitative information of a specific analyte. The word *biosensor* may be used as an acceptable shortened term (16).

In 1991, the International Union of Pure and Applied Chemistry (IUPAC) published a definition and classification of a chemical sensor:

*“ A chemical sensor is a device that transforms chemical information, ranging from the concentration of a specific sample component to total composition analysis, into an analytically useful signal. The chemical information, mentioned above, may originate from a chemical reaction of the analyte or from a physical property of the system”*

In 1996, the Physical Chemistry and Analytical Division of IUPAC proposed their own definition applicable to electrochemical biosensors:

*“ A biosensor is a self-contained integrated device that is capable of providing specific quantitative or semi-quantitative analytical information using a biological recognition element (biochemical receptor) which is in direct spatial contact with a transduction element”*

##### 2.1.1 Basic Components

There are two essential components for a biosensor, an energy transducer and a molecular selective chemical component (biochemical receptor). The basic design for a general biosensor is illustrated in Figure 2.1.

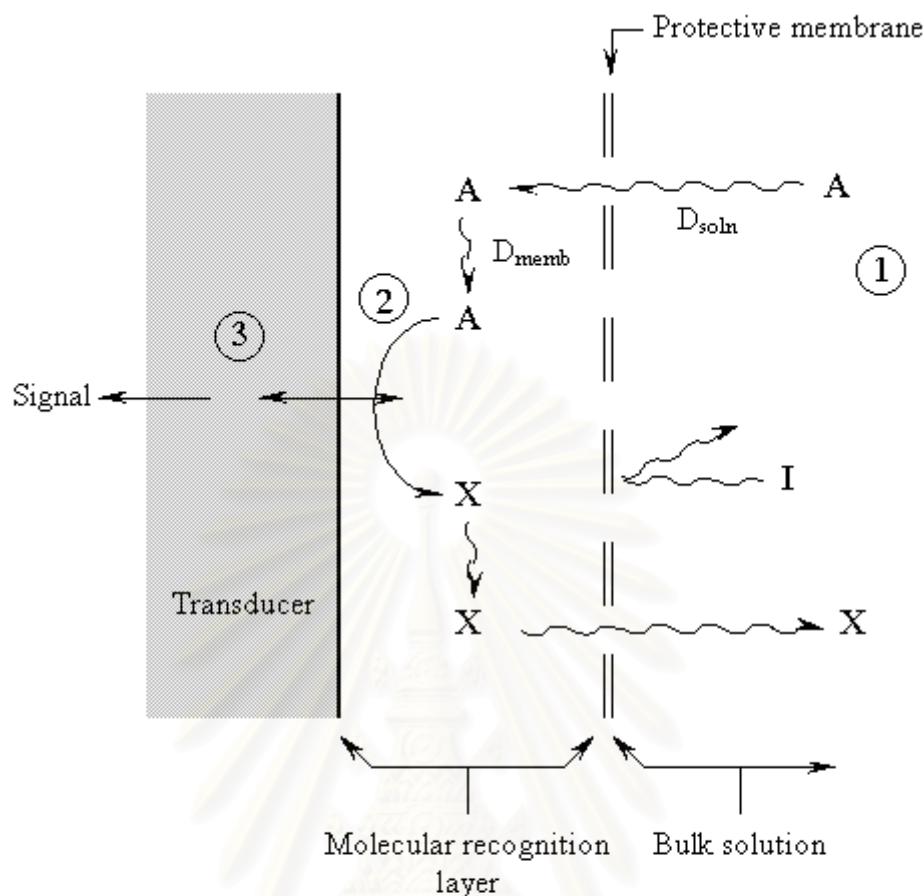


**Figure 2.1** Schematic of a generalized biosensor design: A, analyte; I, Interference; X, product of reaction in the membrane;  $D_{\text{soln}}$ , Diffusion coefficient of A in the solution;  $D_{\text{memb}}$ , Diffusion coefficient of A in the membrane. 1 = Mass transport processes, 2 = Electron transfer process and 3 = Energy transduction process

สถาบันวิทยบริการ  
จุฬาลงกรณ์มหาวิทยาลัย

The energy transducer is modified with a molecular sensitive layer applied to the surface which serve as a permselective or protective membrane. Analytes and interferences migrate to the assembly by one of several mass transport processes – e.g., stirring, flowing stream, diffusion. Analyte partitions into and permeates the membrane or bind to a complementary molecular component. A molecular

recognition event produces the detectable species, which is responsible for signal generation. Diffusion in the membrane differs from diffusion in the sample.

Chemical transduction occurs on or within the sensitive membrane. The selectivity of the sensor depends on the different properties between analyte and interference in term of the chemical reaction and permeability.

The molecular selective chemical component of a biosensor is a biological element such as an enzyme, an immunochemical species, cell or tissues.

### 2.1.2 Energy Transduction Modes

The word, transducer, comes from the Latin word *transducere* which means to lead across. The function of a transducer is to lead across the chemical information of analyte, which can be processed as an electrical signal for data acquisition and interpretation. For example, a phototube transduces light into an electrical signal, which can be recorded by a recorder or computer. This would represent an energy transduction process of any instrumental method. The sensitive layer was merely converted by chemical means (i.e., an ordinary detector) into a more selective detector. The total transducing function of a biosensor is a combination of chemical transduction and energy transduction.

### 2.1.3 Immobilization of Biological Element

#### 2.1.3.1 Adsorption

Adsorption of a biological element has been used for a variety of sensor designs. These macromolecules adsorb on the material of the transducer e.g., metal, metal oxide as well as carbon and glasses. The simplicity of direct surface adsorption of macromolecules for immobilization must be weighed against disadvantages from the problem of subsequent desorption. The problem of non-specific adsorption of unwanted species is also still a problem.

### 2.1.3.2 Entrapment and Cross-linking

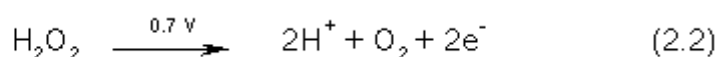
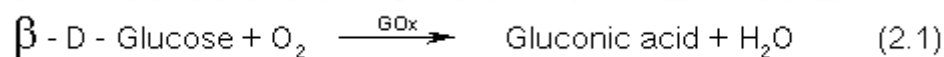
Entrapment and cross-linking of recognition elements and auxiliary reactants in a polymeric network are significant methods. Polymeric matrices range from the gel used as a biological medium to a variety of organic polymers. Several methods are used to produce the film on the transducer such as electrochemical, photochemical, or plasma polymerization methods. A polymeric membrane serves strictly as a structural framework in which the bioselective components are enmeshed, and reduces the leakage and desorption of the reactants. In some cases, the polymeric material may serve additional functions, such as selective ion permeability, enhancement of electrochemical conductivity, or mediation of electron transfer.

### 2.1.3.3 Covalent Attachment

Covalent attachment of a bioselective component is a well-developed approach. As enzymes, antibodies, carbohydrates and oligonucleotides have class-specific molecular characteristics, general approaches for each class have been devised. Compared to adsorption and some entrapment technique, covalent binding often produces a better design of surface structure that enhances the amount of reactant on the surface.

### 2.1.4 Amperometric Glucose Sensors

An amperometric glucose sensor measures the current that is generated by an increase of hydrogen peroxide or decrease of oxygen at a fixed potential. Glucose oxidase (GOx), often require oxygen as an electron acceptor, and is used the amperometric glucose sensor which oxidizes glucose to gluconic acid.



The solubility of oxygen causes a problem at high substrate concentrations because it limits the linear range of the sensor. The regenerated oxygen from hydrogen peroxide at the electrode surface is not enough to meet the demands of the enzymatic reaction, especially at high substrate concentrations.



At the potential, substrates such as ascorbic acid, acetaminophen and uric acid can interfere with the measurement and be a cause of a positive error. The lower range of potentials are used to minimize this interfere. Using redox mediators can solve all these problems.

## 2.2 Electrochemical Methods

### 2.2.1 Fundamental Concepts

#### 2.2.1.1 Faradaic Processes

The measurement of a current response that is related to the concentration of a sample is the objective of controlled-potential electroanalytical experiment (17). This objective is achieved by monitoring the transfer of one or more electrons during the redox process of the analyte. A simple electron transfer reaction can be denoted by:



where O and R are the oxidized and reduced forms of the redox couple, respectively. This process will occur in the potential region that makes the electron transfer thermodynamically or kinetically favorable. For the systems controlled by the laws of thermodynamics, the correlation between the electrode potential and the concentration of the electroactive species at the surface can be described by the Nernst equation:

$$E = E^0 + \frac{2.3RT}{nF} \log \frac{C_O(0, t)}{C_R(0, t)} \quad (2.4)$$

where  $E^0$  is the standard potential for the redox reaction. R is the universal gas constant ( $8.314 \text{ JK}^{-1}\text{mol}^{-1}$ ),  $T$  is the Kelvin temperature,  $n$  is the number of electrons transferred in the reaction, and  $F$  is the Faraday constant (96,487 coulombs). The current resulting from the change in oxidation state of the electroactive species is termed the *faradaic current* because it follows Faraday's law. The current can be plotted vs. the applied potential to give current-potential plot, known as the *voltammogram*.

### 2.2.1.2 Electrical Double Layer

In electrochemistry the array of charged particles and oriented dipoles at the electrode-solution interface due to the potential applied to the electrode is called the electrical double layer. Since the interface must be neutral, a counter-layer is made of an ion with the opposite charge to the electrode. The closest layer to the electrode, known as the inner Helmholtz plane (IHP) contains solvent molecules and specifically adsorbed ions. The imaginary plane passing through the center of the solvated ions at the closest layer to the surface is called the outer Helmholtz plane (OHP). The solvated ions are nonspecifically adsorbed and are attracted to the surface by coulombic force. The combination of both Helmholtz planes is called the compact layer.

The outer layer which extends from the OHP into the bulk solution is known as a diffusion layer. The potential gradient with distance becomes linear from the electrode surface to the OHP and then exponentially in the diffusion layer.

The electrical double layer has a similarity to the parallel – plate capacitor. For an ideal capacitor, the charge ( $q$ ) is directly proportional to the potential difference.

$$q = CE \quad (2.5)$$

Where  $C$  is the capacitance (F). The potential charge relationship for the electrical double layer is

$$q = C_{dl}A(E - E_{pzc}) \quad (2.6)$$

When  $C_{dl}$  is the capacitance per unit area and  $E_{pzc}$  is the potential of zero charge. Capacitance of double layer consists of the capacitance of the compact layer and diffusion layer. The total capacitance is given by

$$1/C = 1/C_H + 1/C_G \quad (2.7)$$

Where  $C_H$  and  $C_G$  represent the capacitance of the compact layer and diffusion layer, respectively. Comparison to a parallel-plate capacitor,  $C_H$  is given by

$$C_H = - \epsilon/4\pi d \quad (2.8)$$

Where  $d$  is the distance between the plate and  $\epsilon$  is the dielectric constant. The compact layer capacitance is generally independent of the electrolyte concentration, most of the charge is arranged near the compact layer, and the rest is scattered diffusely into the bulk solution. These conditions cause  $C_G$  to have a

value greater than  $C_H$ ,  $1/C_H \gg 1/C_G$ , or  $C \sim C_H$ . On the other hand, the low electrolyte concentrations,  $C_G$  value is smaller than  $C_H$ , causing  $C \sim C_G$ . The schematic diagram of an electrical double layer is illustrated in Figure 2.2.

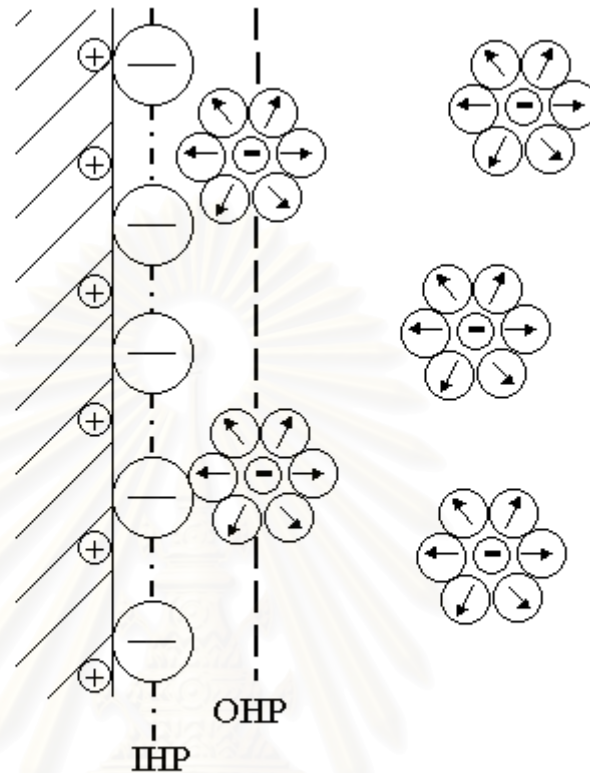


**Figure 2.2** Schematic diagram of the electrical double layer.

### 2.2.1.3 Mass Transport

Mass Transport occurs by three different modes:

- i) diffusion: the spontaneous movement under the influence of a concentration gradient. (i.e., from high concentration region to lower concentration region);
- ii) convection: transport occurs by a physical movement; such as hydrodynamic motion of the solution or because of density gradients; and
- iii) migration: transport of charged particles under the influence of an electric field

The common measurement of the rate of mass transport at the fixed points is the flux ( $J$ ). It is defined as the number of molecules penetrating a unit area of an imaginary plane in a unit of time. The flux to the electrode is described by a differential equation, known as the Nernst-Planck equation, given here:

$$J(x, t) = -D \frac{\partial C(x, t)}{\partial x} - \frac{zFC}{RT} \frac{\partial \phi(x, t)}{\partial x} + C(x, t)V(x, t) \quad (2.9)$$

Where  $D$  is the diffusion coefficient ( $\text{cm}^2 \text{s}^{-1}$ ),  $\frac{\partial C(x, t)}{\partial x}$  is the concentration gradient (at distance  $x$  and time  $t$ ),  $\frac{\partial \phi(x, t)}{\partial x}$  is the potential gradient,  $z$  and  $C$  are the charge and concentration, respectively, of the electroactive species, and  $V(x, t)$  is the hydrodynamic velocity (in the  $x$  direction). In aqueous media,  $D$  usually ranges between  $10^{-5}$  and  $10^{-6} \text{cm}^2 \text{s}^{-1}$ . The current ( $i$ ) is directly proportional to the flux:

$$i = -nFAJ \quad (2.10)$$

where  $A$  is the electrode area.

As indicated by equation 2.9, a quite complex situation is apparent when the three modes of mass transport occur simultaneously. This complication makes it difficult to relate the current to the analyte concentration. The situation can be simplified by suppressing electromigration and convection. The effect of electromigration can be suppressed by the addition of excess inert salt (supporting electrolyte). Normally, a supporting electrolyte present at  $\sim 0.1 \text{ M}$ , which reduces the solution resistance between electrodes, does not interfere with the electrode reaction. Moreover, the addition of supporting electrolyte will dissipate the electric field distribution in solution uniform. Operation in a quiescent solution and measurement over relatively short time can decrease the convection effect. Under these conditions, the movement of the electroactive species is controlled by diffusion. Equations governing diffusion processes are thus pertinent to many electroanalytical techniques.

The rate of diffusion is directly proportional to the slope of the concentration gradient. Thus, Fick's first law is introduced:

$$J(x, t) = -D \frac{\partial C(x, t)}{\partial x} \quad (2.11)$$

Substitution of equation 2.10 in equation 2.11 yields a general expression for the current response:

$$I = nFAD \frac{\partial C(x, t)}{\partial x} \quad (2.12)$$

As indicated by the equation above, the current is proportional to the concentration gradient of the electroactive species. The diffusional flux is time dependent. The variation in concentration with time due to diffusion is described by Fick's second law (for linear diffusion):

$$\frac{\partial C(x, t)}{\partial t} = D \frac{\partial^2 C(x, t)}{\partial x^2} \quad (2.13)$$

Fick's laws explain the flux and the concentration of the electroactive species as functions of position and time. These partial differential equations can be solved by the application of a mathematical method. The Laplace transformation is the technique to be applied (18).

### 2.2.2 Controlled-Potential Technique

The basis of all controlled-potential techniques is the measurement of the current response to an applied potential of the electrode. These techniques can be used for qualitative and quantitative determination and for kinetic and thermodynamic studies

### 2.2.2.1 Cyclic Voltammetry

Cyclic voltammetry is a technique involving the measurement of current–potential relationships. The potential is varied linearly with time along a triangular waveform in a quiescent solution. The current–potential curve, known as the voltammogram, is governed by the rate of electron transfer across the electrode–solution interface as shown in figure 2.3.

As the electrode potential is changed in the positive direction, the reductant begins to be oxidized. The electron flow from solution to the working electrode and an oxidation current can be observed ( $i_{pa}$ ). For the opposite process, as the electrode potential is then moved in a negative direction, the reduction process occurs and the surface concentration of “O” decreases. The electrons flow back from the electrode to the solution, so a reduction current can be observed ( $i_{pc}$ ). In each case, if the potential is moved far enough,  $i_{pa}$  and  $i_{pc}$  will reach a peak and then decrease. This is because the rate of electron transfer is now faster than the mass transport. The decrease in “O” is coupled with an increase in the diffusion layer thickness, yielding a peak-shaped voltammogram as shown in figure 2.4.

### 2.2.2.2 Amperometry

Amperometry is a technique that involves the measurement of current–time relationships. The potential is kept constant and the current is recorded as a function of time. The resulting current is a linear function of the concentration of the electroactive species from equation.

$$i_d = \frac{nFADC}{\delta} \quad (2.14)$$

where  $n$  = number of electron transfer

$F$  = Faraday constant (C/mol)

$D$  = Diffusion coefficient (cm<sup>2</sup>/s)

$A$  = Electrode area (cm<sup>2</sup>)

$C$  = Concentration of reactant in bulk solution (mol/cm<sup>3</sup>)

$\delta$  = Nernst diffusion layer (cm)

## 2.3 Flow Injection Analysis (FIA)

Flow injection analysis (FIA) is based on the injection of a liquid sample into a moving carrier stream of a suitable liquid. The injected sample forms a zone, which is then moved toward a detector that continuously records the signal response as the base line changes due to the passage of the sample through the flow cell(19).

### 2.3.1 Flow Amperometry

Electrochemical detection in a flowing system is usually performed by controlling the potential of the working electrode at a constant value and recording the current as a function of time. This technique is called flow amperometry. The current response reflects the concentration profiles of the electroactive species as they pass through the detector. Detection for flow injection system results in sharp current peak. The magnitude of the peak current corresponds to the concentration.

### 2.3.2 Mass Transport and Current Response

Well-define hydrodynamic conditions, with high rate of mass transport, are essential for the useful of electrochemical detector. According to the Nernst approximation, the diffusion layer thickness ( $\delta$ ) is empirically related to the solution flow rate ( $U$ ) as follow:

$$\delta = BU^\alpha \quad (2.15)$$

where  $B$  and  $\alpha$  are constant for a given set of conditions. Substitution of equation 2.15 in the general current response for mass transport-controlled reaction ( $i_t = nFADC/\delta$ ) yield the limiting steady-state response of flow through electrode

$$i_t = nFAK_m CU^\alpha \quad (2.16)$$

where  $K_m$  is the mass-transport coefficient ( $D/B$ ).

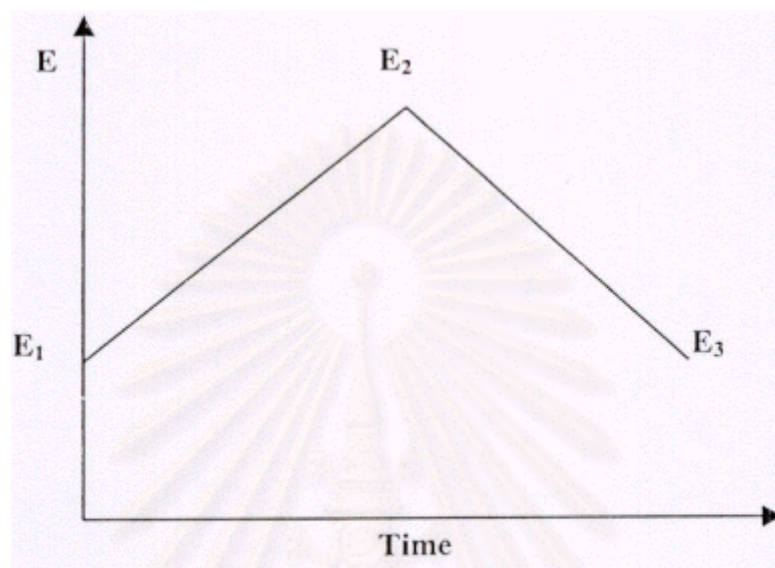


**Figure 2.3** Triangular waveform for cyclic voltammetry.  
Where  $E_1$  = initial potential  
 $E_2$  = switching potential  
 $E_3$  = final potential

สถาบันวิทยบริการ  
จุฬาลงกรณ์มหาวิทยาลัย



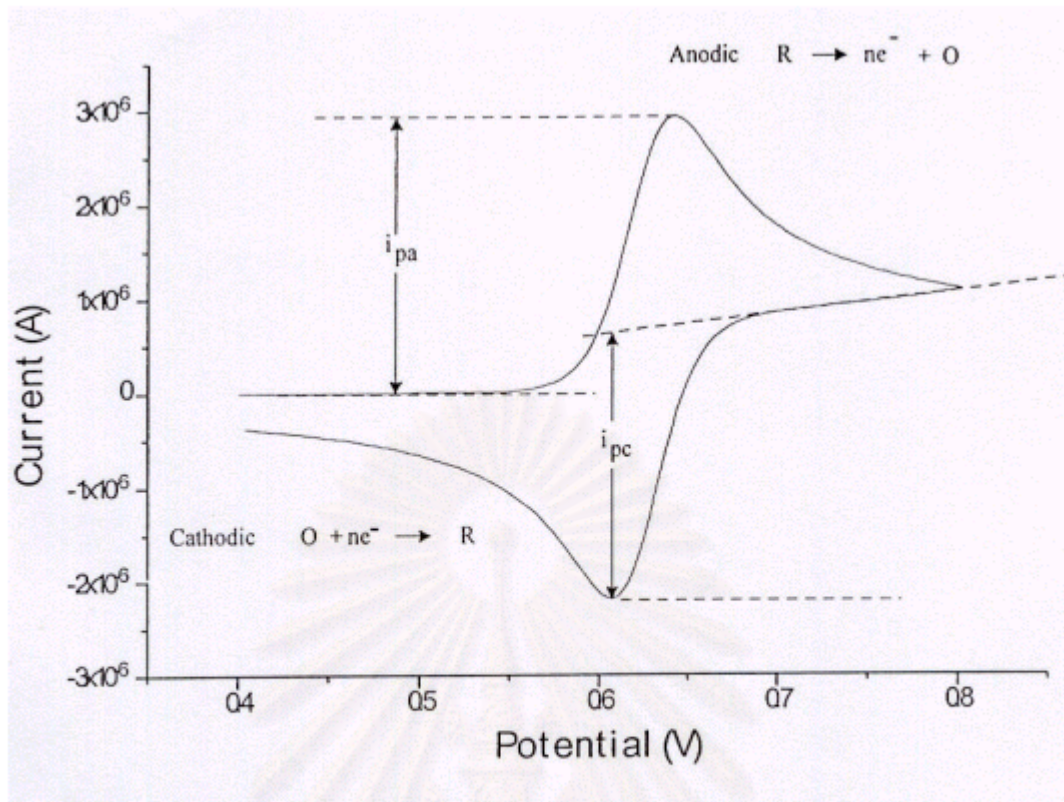


**Figure 2.4** A typical cyclic voltammogram for reversible process

สถาบันวิทยบริการ  
จุฬาลงกรณ์มหาวิทยาลัย

## CHAPER III

### EXPERIMENTAL

#### 3.1 Apparatus

All electrochemical experiments were conducted with the PGSTAT10 Autolab potentiostat and controlled by GPES 4.4 software (EcoChemie, the Netherlands). The electrode polishing kit was manufactured from BAS (Bioanalytical Systems, USA.). The buffer pH was measured by the 774 pH meter (Metrohm, Switzerland). The water used in all experiments was supplied by the reverse osmosis system (RiOs 8, model Millipore ZROS5008Y, with Automatic Sanitization Module, Millipore, USA.). The three-electrode system was used in all experiments.

##### 3.1.1 Electrode Modification

- a) Working electrode, gold foil (4 mm diameter, 0.25 mm thickness) with percent purity > 99.99%, Goodfellow, England
- b) Ag/AgCl Reference electrode, Bioanalytical Systems, USA.
- c) Counter electrode, platinum
- d) Ultrasonic bath, ULTRASONIK CLEANER Model 28H, NeyDental Inc., USA.
- e) P2 micro-autopipette (adjustable volume), Gilson, France
- f) P20 micro-autopipette (adjustable volume), Gilson, France
- g) P200 micro-autopipette (adjustable volume), Gilson, France
- h) P5000 autopipette (adjustable volume), Gilson, France
- i) Vacuum distillation equipment

### 3.1.2 The FIA Experiments

- a) Working electrode, enzyme-modified gold electrode (obtain from Section 3.1.1)
- b) Ag/AgCl reference electrode, Bioanalytical Systems, USA.
- c) Counter electrode, platinum foil (4 mm diameter, 0.125 mm thickness) with percent purity > 99.99%, Goodfellow, England
- d) Liquid flow cell, homemade
- e) Model 5020 low-pressure sample injection valve (6 port valve) with 100  $\mu$ L sample loop and Luer Hub connector, Rheodyne, USA.
- f) 1 mL plastic syringes for Luer Hub connector, Alltech, USA.
- g) Teflon tubing (1/16" OD x 0.030" ID), Alltech, USA.
- h) PEEK fingertight fitting for 1/16" flanged tubing, Alltech, USA.
- i) Pipe plugs (1/8"), Cole-Parmer Instrument Company, USA.
- j) EASY-FLANGE™, flange rolling tool, Alltech, USA.
- k) Tygon pump tubing (0.0812" ID), Cole-Parmer Instrument Company, USA.
- l) Peristaltic pump (8 channel), Ismatec, Switzerland



Figure 3.1 Gold disk electrodes

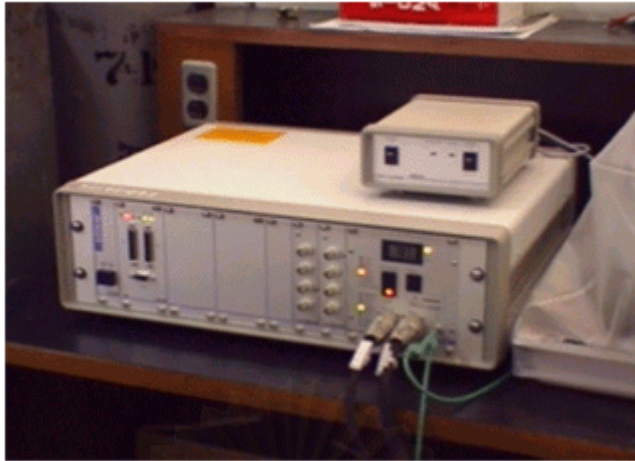


Figure 3.2 PGSTAT10 Autolab potentiostat

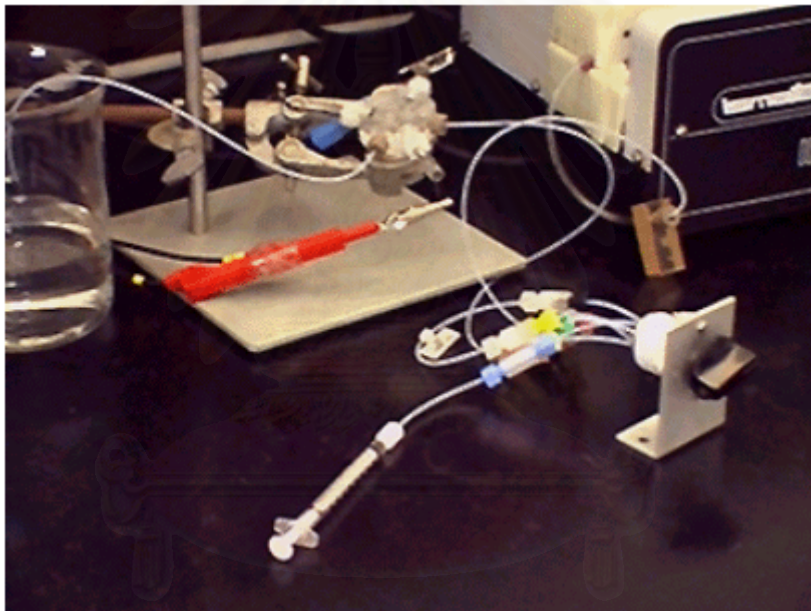


Figure 3.3 Flow injection system

สถาบันวิจัยบริการ  
จุฬาลงกรณ์มหาวิทยาลัย

### 3.2 Chemicals

- a) Enzyme glucose oxidase (EC 1.1.3.4) from *Aspergillus niger*, Sigma, England
- b) Nafion<sup>®</sup> 117 Solution, purum, Fluka, England
- c) Hexaammine ruthenium (III) chloride, 95% purity, Aldrich, England
- d) Pyrrole, 97% purity (zer Synthese), Merck, Germany
- e) D (+) Glucose anhydrous, RPE-ACS, Farmitala Carlo Erba, Italy
- f) Disodium hydrogen phosphate, A.R., Riedel-de Haen, Germany
- g) Potassium dihydrogen phosphate, pro analysi, Merck, Germany
- h) Potassium ferricyanide, pro analysi, Merck, Germany
- i) Potassium chloride, pro analysi, Merck, Germany
- j) L (+) Ascorbic acid, pro analysi, Merck, Germany
- k) Acetone, pro analysi, Merck, Germany
- l) Hydrochloric acid, AnalaR, BDH, England
- m) Nitric acid, AnalaR, BDH, England
- n) Sulfuric acid, AnalaR, BDH, England

### 3.3 Fabrication of Disk Electrode

Gold foil (4 mm diameter) connected to silver wire with electroconductive glue and sealed in glass tube (4 mm ID x 6 cm) with epoxy resin, as shown in Figure 3.1, was used as working electrode in all experiments (see Appendix A). The electrode was polished by white nylon-polishing pad with a few drops of 1  $\mu\text{m}$  diamond slurry. The electrode was placed face down on the pad and polished using a smooth motion with even pressure. After 1-2 minutes, the electrode was removed, rinsed and sonicated in deionized water for 5 minutes. Next, the electrode was polished again using the microcloth-polishing pad with several drops of 0.3  $\mu\text{m}$  polishing alumina. The electrode was polished with the same manner as in the previous step. After that, the electrode was rinsed then sonicated in deionized water removed water.

Electrochemical cleaning of gold disk electrode was performed using cyclic voltammetry in 0.1 M sulfuric acid. The sweeping potential is between  $-0.2$  to  $1.6$  V (vs. Ag/AgCl reference electrode) with a scan rate  $0.1$  V/s (about 20 cycles). Next, all the electrodes were removed and then rinsed well with deionized water. This electrochemical-cleaning step must be done every time before used.

The platinum disk electrode (platinum foil, 4 mm in diameter) was constructed and polished in the same manner as gold disk electrode but no need to do the electrochemical-cleaning step. This platinum disk electrode was served as counter electrode in the FIA experiments.

### 3.4 Fabrication of Flow Cell

In this research, all flow cells used in flow experiment were made from acrylic. The first configuration, *flow cell I*, was fabricated to support the three-electrode system. Figure 3.4 shows the position for working electrode (glucose sensor), reference electrode, counter electrode as well as inlet and outlet. The diameter of inner channel between these electrodes was 1 mm. The electrodes were fitted to the flow cell using O-ring and paraffin tape. Inlet and outlet was sealed with silicone adhesive.

In *flow cell II*, the angle of counter electrode was decrease about 45 degree lower from the horizontal plane as shown in Figure 3.5. In this manner, the stagnant effect can be reduced due to the gravitation force. This cell structure provides a sharp peak but the leakage still remain.

The finger tight nuts and adapter fitting accessories were used to fabricate the *flow cell III* as shown in Figure 3.6. Moreover, the inner channel diameter and the distance between all electrodes were reduced in order to minimize the dispersion of sample in the flow cell.

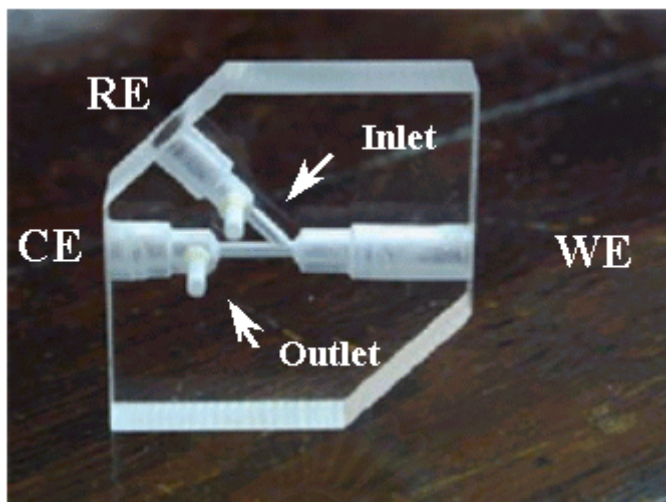


Figure 3.4 The flow cell I, WE = Working electrode,  
RE = Reference electrode and CE = Counter electrode

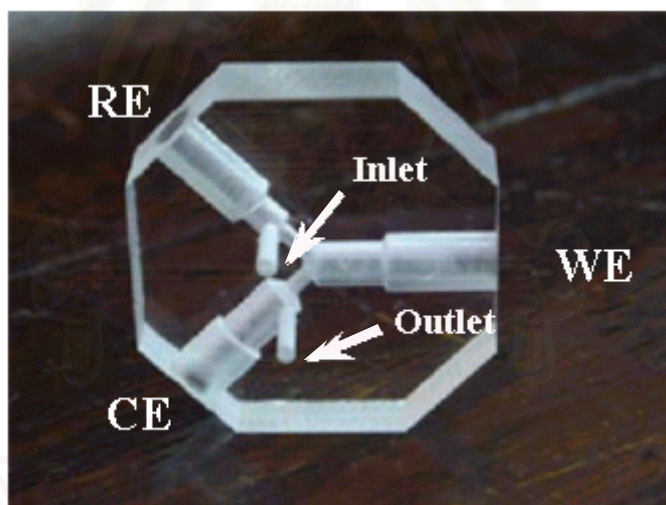


Figure 3.5 The flow cell II, WE = Working electrode,  
RE = Reference electrode and CE = C

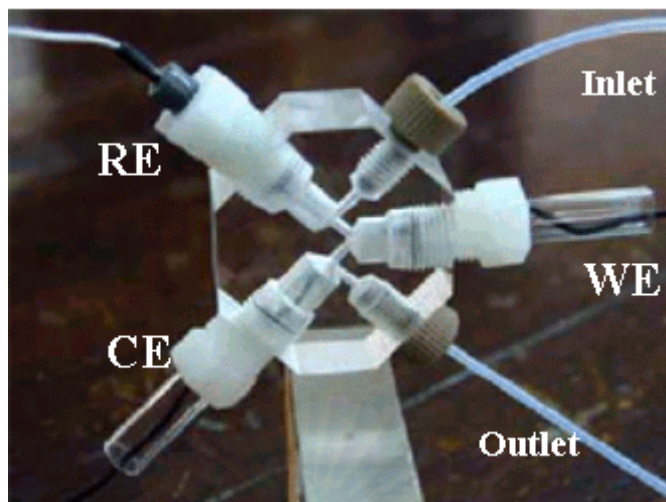


Figure 3.6 The flow cell III with all electrodes. WE = Gold disk electrode, RE = Ag/AgCl reference electrode and CE = Platinum disk electrode.

### 3.5 Preparation of Amperometric Glucose Sensor

#### 3.5.1 Surface Pretreatment

Electrochemical cleaning of gold electrode was performed in 0.1 M  $\text{H}_2\text{SO}_4$  using cyclic voltammetry. Prior to the electropolymerization step, the electrode potential was swept three times between  $-0.7$  to  $0.7$  V vs. Ag/AgCl at scan rate of  $0.1$  V/sec in phosphate buffer solution, to ensure the reproducible surface.

#### 3.5.2 Surface Modification

##### *Procedure I*

Approximate  $1 \mu\text{L}$  of Nafion solution was added onto the electrode surface and by dropping and allowed to dry for 10 minutes and a Nafion electrode is obtained. After that the Nafion-modified electrode was dipped into  $\text{Ru}(\text{NH}_3)_6\text{Cl}_3$  solution for 10 minutes in order to provide electrostatic binding. The  $\text{Ru}(\text{NH}_3)_6\text{Cl}_3$  concentration was varied over the wide range ( $10$  mM –  $50$  mM). The electrode that prepared in this step was so-called  $\text{Ru}(\text{NH}_3)_6\text{Cl}_3$ -Nafion modified electrode. This electrode was served as working electrode in the electropolymerization step.



Electropolymerization was performed in one compartment cell at room temperature. The electrodeposition solution was comprised of different amounts of pyrrole monomer and enzyme with total volume of 5 mL. The pyrrole monomer was added into 0.1 M phosphate buffer solution (pH 7.0) and stirred for about 60 seconds to dissolve all of the monomers. Then the enzyme was added in the resulting solution. Films were grown potentiostatically at 0.7 V (vs. Ag/AgCl) in quiescent solutions. The film thickness was fixed at 0.3  $\mu\text{m}$ , assume that 45  $\text{mC}/\text{cm}^2$  of charge yield 0.1  $\mu\text{m}$  thickness. After the electropolymerization, the electrode was sonicated in 0.1 M phosphate buffer solution for 1 minute to remove weakly adsorb enzyme and unreacted monomer. The electrode was kept in 0.1 M phosphate buffer solution at a temperature less than 4°C, (when not in use).

#### *Procedure II*

Electropolymerization was performed in 0.1 M KCl containing pyrrole monomer, glucose oxidase and  $\text{Ru}(\text{NH}_3)_6\text{Cl}_3$ . The Nafion-coated electrode was immersed into growth solution for 10 minutes in order to bind with  $[\text{Ru}(\text{NH}_3)_6]^{3+}$ . The film was formed potentiostatically at 0.7 V (vs. Ag/AgCl) in unstirred solutions. The degree of polymerization was varied to provide the desire film thickness. After the electropolymerization, the electrode was sonicated in 0.1 M phosphate buffer solution for 1 minute to remove weakly adsorb enzyme and unreacted monomer. The electrode was kept in 0.1 M phosphate buffer solution at a temperature less than 4°C, (when not in use).

### 3.6 Investigation of $[\text{Ru}(\text{NH}_3)_6]^{3+}$ in the Polymerized Film

The cyclic voltammogram of the modified sensor in 0.1 M phosphate buffer solution indicated that  $[\text{Ru}(\text{NH}_3)_6]^{3+}$  can be entrapped in the films. Figure 4.9 shows the cyclic voltammogram for oxidation-reduction of  $[\text{Ru}(\text{NH}_3)_6]^{3+}$  in the polypyrrole film.

### Electrode Surface

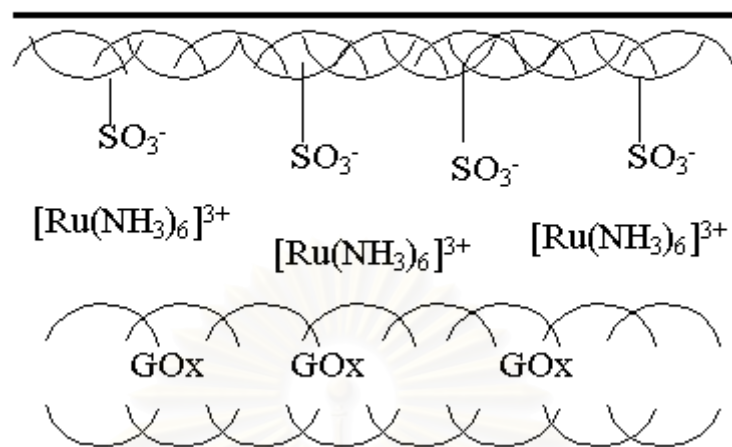


Figure 3.7 Schematic diagram of the modified sensor obtained from procedure I (GOx = Glucose oxidase).

### Electrode Surface

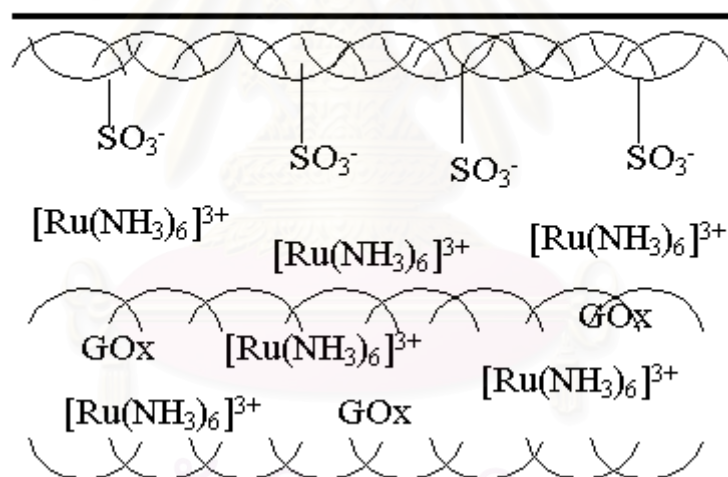


Figure 3.8 Schematic diagram of the modified sensor obtained from procedure II (GOx = Glucose oxidase).

### 3.7 Determination of Glucose using FIA system

The amperometric response of glucose was determined using FIA system. All three electrodes were mounted to the homemade flow cell. Phosphate buffer solution was used as carrier stream. The concentration of phosphate was 0.1 M (pH 7.0). The flow rate was varied to investigate the optimum peak shape and sampling rate. After applying the potential, the background current was allowed to be constant. Then glucose solution was injected using injection port with 100  $\mu$ L sample loop.

### 3.8 Interference Studies

Ascorbic acid and acetaminophen were used as interferences in these studies. The current responses of 2 mM ascorbic acid and 2 mM acetaminophen obtained from the modified sensor was compared with unmodified electrode.



สถาบันวิทยบริการ  
จุฬาลงกรณ์มหาวิทยาลัย

## CHAPTER IV

### RESULTS AND DISCUSSION

#### 4.1 Optimum Flow Cell Structure

The flow cell characteristic was investigated using bare gold electrode. The first configuration, *flow cell I*, provides the tailing peak due to the dead volume close to working and counter electrode as shown in Figure 4.1 and 4.2. Moreover, the leakage was found at the connection between cell and electrodes especially at high flow rate.

*Flow cell II*, the tailing effect due to the dead volume could be minimized by decreasing the angle of the counter electrode by about 45 degrees below the horizontal plane as shown in Figure 4.3 and 4.4. In this manner, the stagnant effect can be reduced due to the gravitation force. This cell structure provides a sharp peak but the leakage still remain.

Both of the flow cells described above have the same problem in term of the leakage. To solve these problems, finger tight nuts and adapter fitting accessories were used to fabricate the *flow cell III*. Moreover, the inner channel diameter and the distance between all electrodes were reduced in order to minimize the dispersion of sample in the flow cell as shown in Figure 4.5 and 4.6. The results obtained from each flow cell were shown in Table 4.1

สถาบันวิทยบริการ  
จุฬาลงกรณ์มหาวิทยาลัย

Table 4.1 Characteristic properties of the fabricated flow cells

Type	Characteristic properties
flow cell I	<ul style="list-style-type: none"> <li>- tailing peak due to the stagnant effect</li> <li>- large area of dead volume</li> <li>- the leakage can be observed</li> </ul>
flow cell II	<ul style="list-style-type: none"> <li>- no stagnant effect</li> <li>- dead volume can be minimized</li> <li>- the leakage can be observed</li> </ul>
flow cell III	<ul style="list-style-type: none"> <li>- no stagnant effect</li> <li>- zero dead volume</li> <li>- no leakage</li> </ul>

#### 4.2 Determination of Glucose in Flow Injection System

##### Procedure I

Determination of glucose in flow experiment was performed using *flow cell III*. Figure 4.10 and 4.11 were shown the signal response to 200 mM glucose at 0.7V and 0.4 V vs. Ag/AgCl, respectively. The conditions were shown in Table 4.2 and Table 4.3.

สถาบันวิทยบริการ  
จุฬาลงกรณ์มหาวิทยาลัย

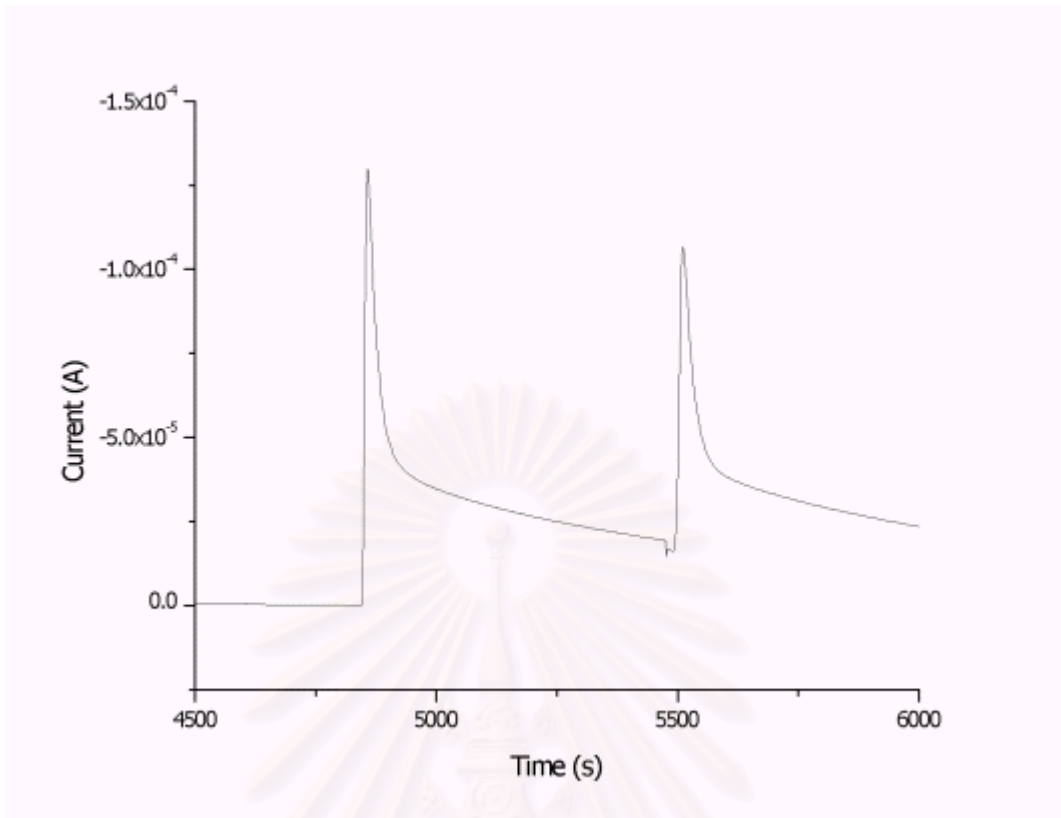


Figure 4.1 Current response to 200 mM  $K_3Fe(CN)_6$  using flow injection system (flow cell I, WE = Bare gold electrode) at 0.25 V vs Ag/AgCl. The injection volume is 100  $\mu$ L, flow rate is 0.7 mL/min.

สถาบันวิทยบริการ  
จุฬาลงกรณ์มหาวิทยาลัย

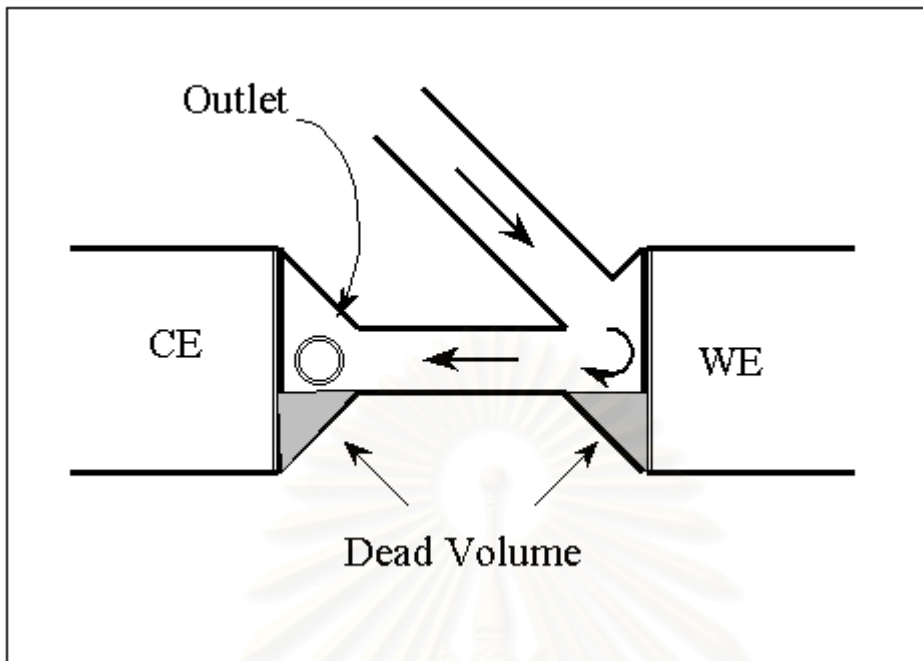


Figure 4.2 Schematic diagram of flow cell I

สถาบันวิทยบริการ  
จุฬาลงกรณ์มหาวิทยาลัย

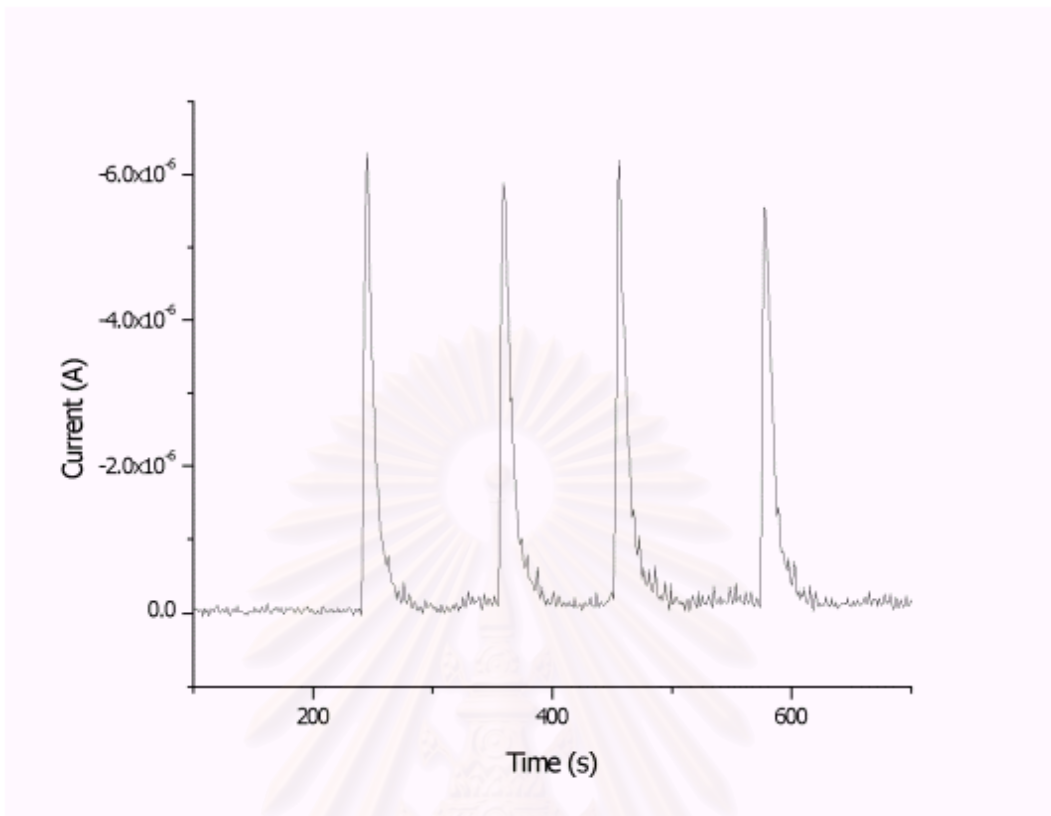


Figure 4.3 Current response to 2 mM  $\text{K}_3\text{Fe}(\text{CN})_6$  using flow injection system (flow cell II, WE = Bare gold electrode) at 0.25 V vs Ag/AgCl. The injection volume is 100  $\mu\text{L}$ , flow rate is 0.7 mL/min.

สถาบันวิทยบริการ  
จุฬาลงกรณ์มหาวิทยาลัย



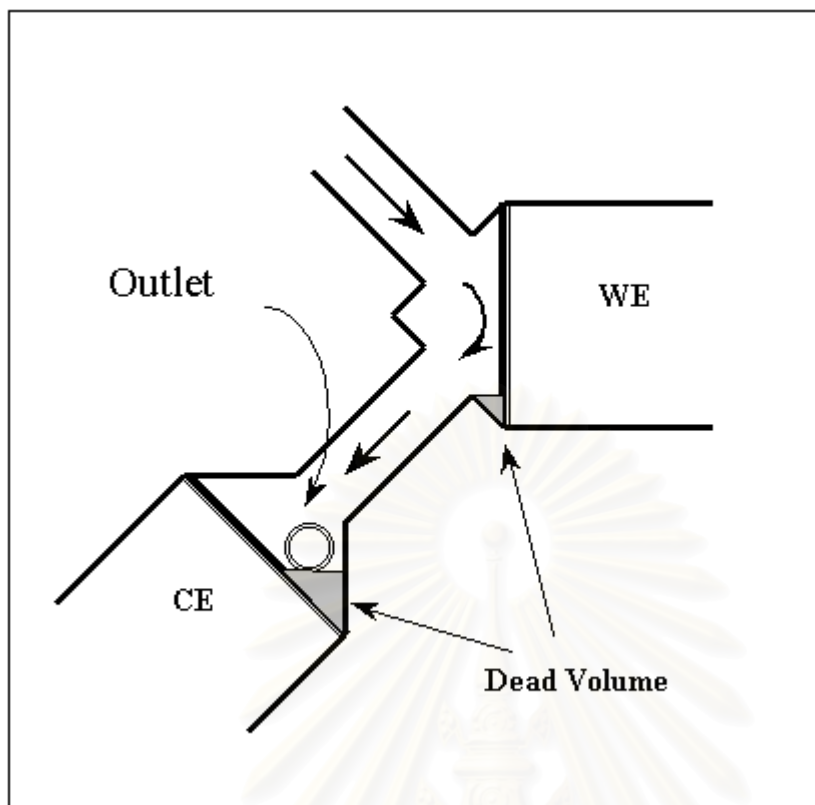


Figure 4.4 Schematic diagram of flow cell II.

สถาบันวิทยบริการ  
จุฬาลงกรณ์มหาวิทยาลัย

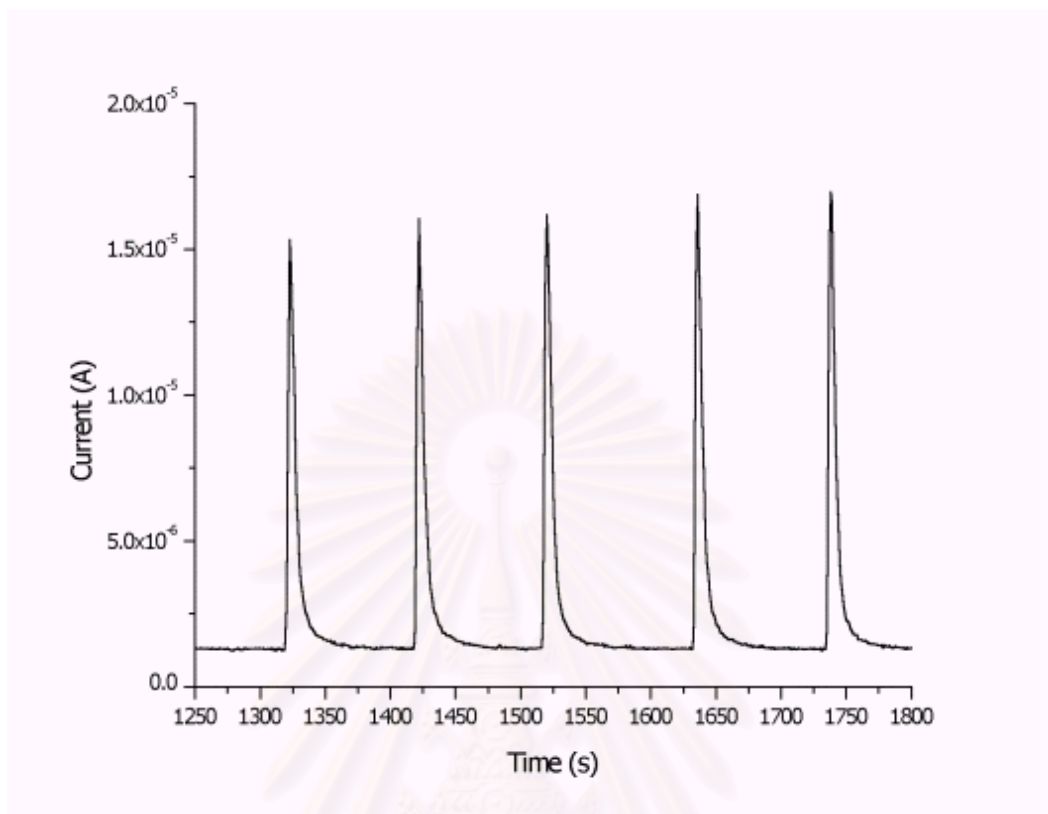


Figure 4.5 Current response to 2 mM ascorbic acid using flow injection system (flow cell III, WE = Bare gold electrode) at 0.4 V vs Ag/AgCl. The injection volume is 100  $\mu$ L, flow rate is 0.7 mL/min.

สถาบันวิทยบริการ  
จุฬาลงกรณ์มหาวิทยาลัย

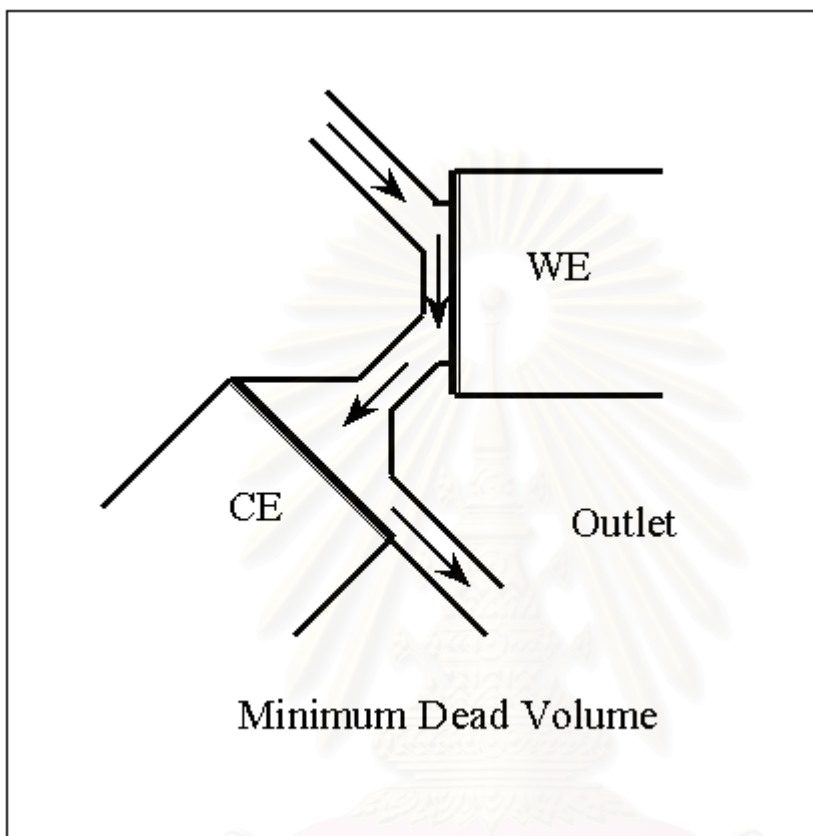


Figure 4.6 Schematic diagram of flow cell III.

สถาบันวิทยบริการ  
จุฬาลงกรณ์มหาวิทยาลัย

**Table 4.2** The conditions for the preparation of glucose sensor (procedure I).

Volume of Nafion in the pre-coating step:	1 $\mu\text{L}$
$\text{Ru}(\text{NH}_3)_6\text{Cl}_3$ solution:	10 mM
Growth solution:	
Phosphate buffer solution	0.1 M
Total volume 5 mL containing	
Pyrrole	0.1 M
glucose oxidase	100 Units/mL
Polymerization potential:	Potentiostatic at 0.7 V
Charge:	17 mC (0.3 $\mu\text{m}$ thickness)

**Table 4.3** The conditions for flow injection system (procedure I).

Flow system:	Single line mode
Flow cell configuration:	<i>Flow cell III</i>
Operating potential for	
determination of glucose:	0.7 and 0.4V vs. Ag/AgCl
Carrier stream:	0.1 M phosphate buffer solution, pH
Flow rate:	7.0
Injection volume of sample:	0.7 mL/min
	100 $\mu\text{L}$

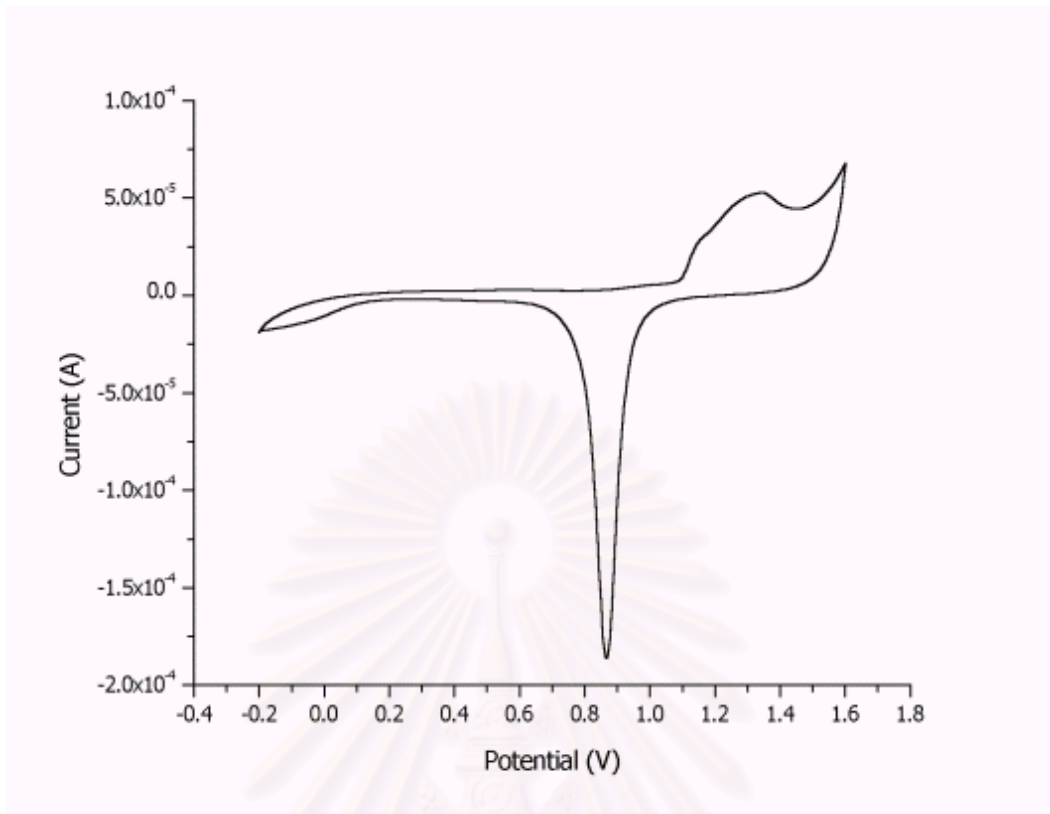


Figure 4.7 Cyclic voltammogram at bare gold in 0.1 M  $\text{H}_2\text{SO}_4$  from -0.2 to 1.6 V vs. Ag/AgCl, scan rate 0.1 V/sec. Counter electrode was platinum

สถาบันวิทยบริการ  
จุฬาลงกรณ์มหาวิทยาลัย

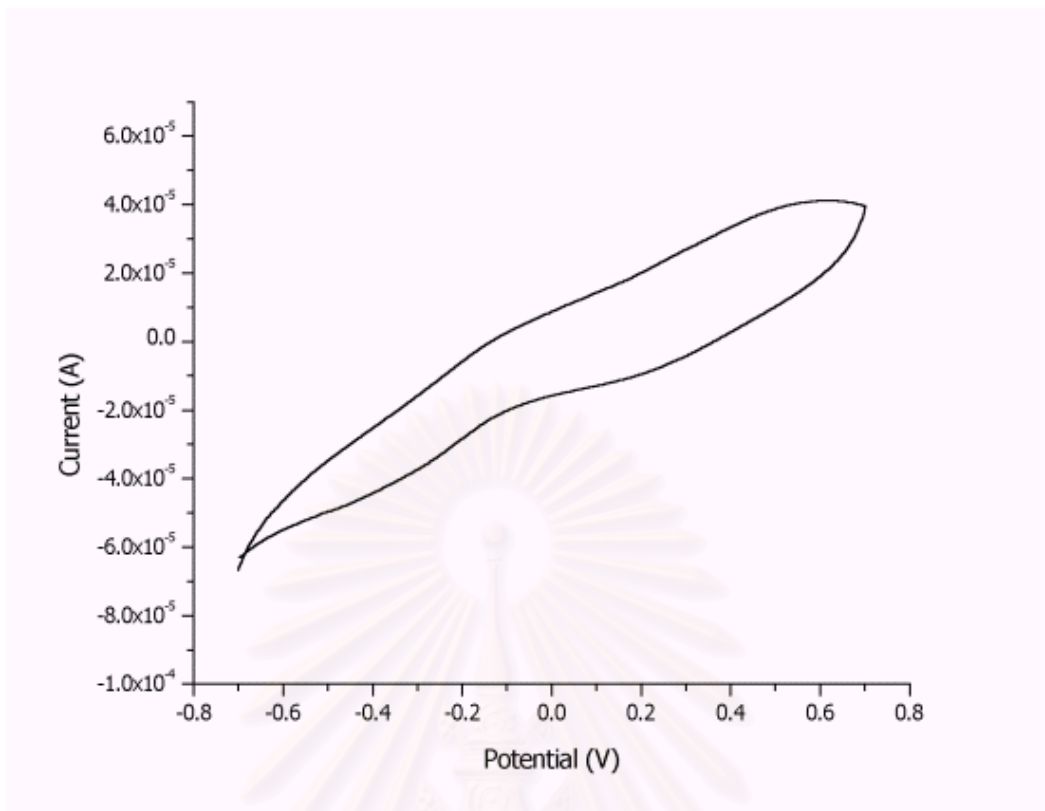


Figure 4.8 Cyclic voltammogram at bare gold in 0.1 M phosphate buffer solution from -0.7 to 0.7 V vs. Ag/AgCl, scan rate 0.1 V/sec. Counter electrode was platinum

สถาบันวิทยบริการ  
จุฬาลงกรณ์มหาวิทยาลัย

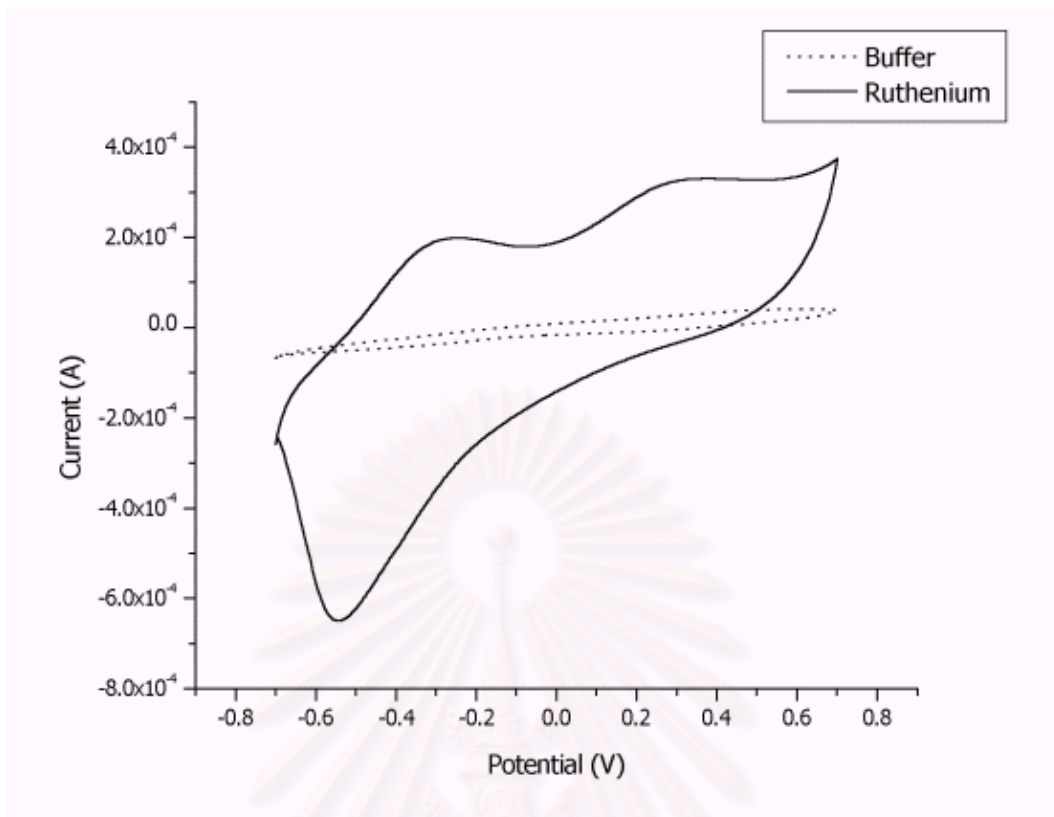


Figure 4.9 Cyclic voltammogram in 0.1 M phosphate buffer solution from -0.7 to 0.7 V vs. Ag/AgCl, scan rate 0.1 V/sec. Counter electrode was platinum. Solid line is oxidation-reduction of  $[\text{Ru}(\text{NH}_3)_6]^{3+}$  and dotted line is background.

สถาบันวิทยบริการ  
จุฬาลงกรณ์มหาวิทยาลัย

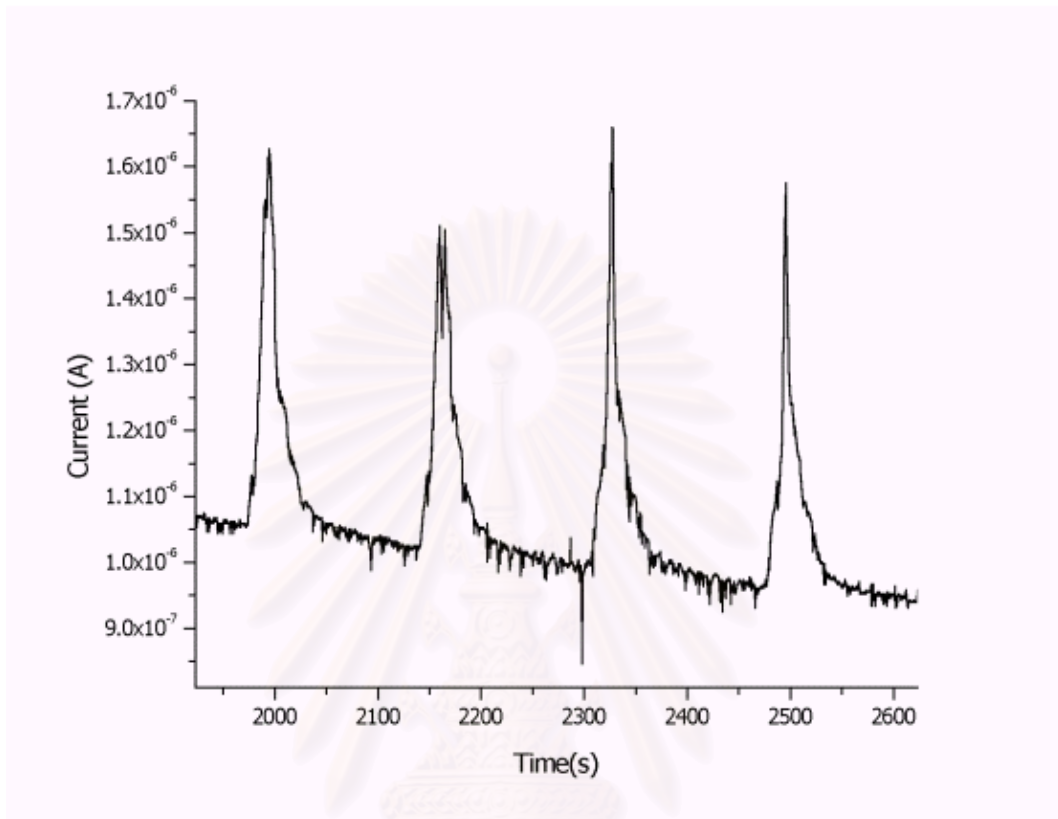


Figure 4.10 Current response to 200 mM glucose using flow injection system at 0.7 V vs Ag/AgCl. The injection volume is 100  $\mu\text{L}$ , flow rate is 0.7 mL/min. (WE = Glucose sensor)

สถาบันวิทยบริการ  
จุฬาลงกรณ์มหาวิทยาลัย



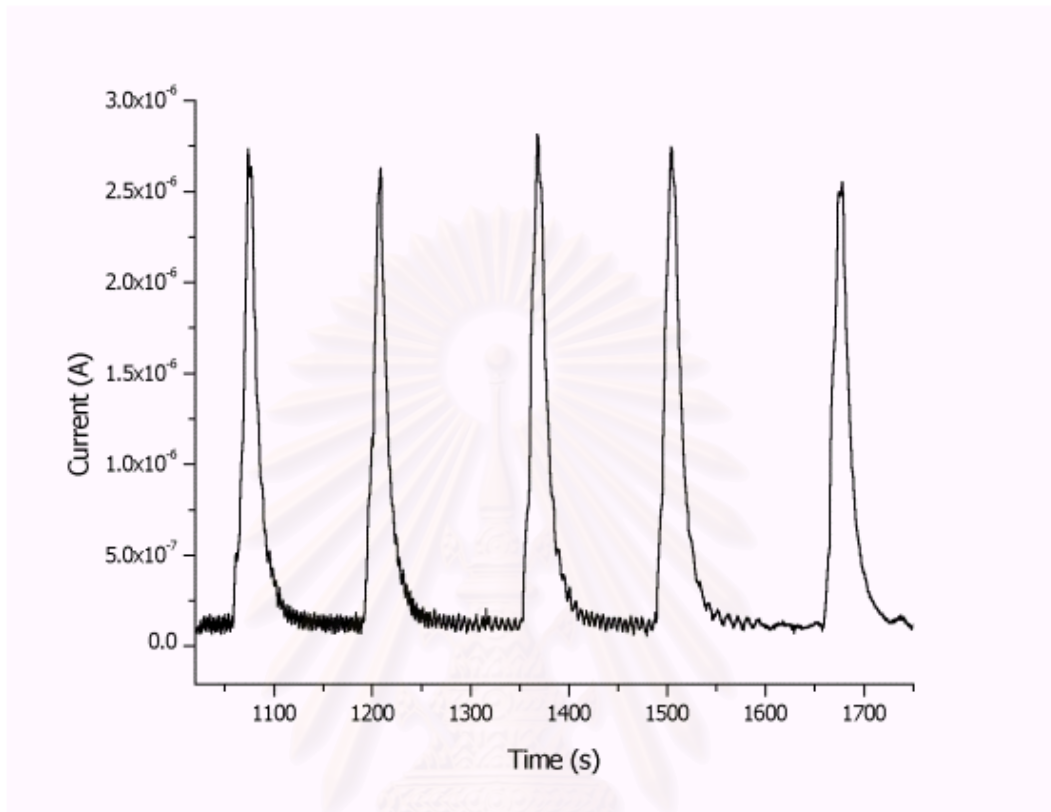


Figure 4.11 Current response to 200 mM glucose using flow injection system at 0.4 V vs Ag/AgCl. The injection volume is 100  $\mu\text{L}$ , flow rate is 0.7 mL/min. (WE = Glucose sensor)

สถาบันวิทยบริการ  
จุฬาลงกรณ์มหาวิทยาลัย

#### 4.2.1 The effect of Carrier Flow Rate

The shape and height of peaks are affected by the flow rate of the carrier stream. Peaks recorded for flow rate ranging from 0.5 to 1 mL/min are shown in Figure 4.12. An increase in flow rate leads to a decrease in signal magnitude. The signal decreased only 10 % when the flow rate was changed from 0.5 to 0.7 mL/min, but decreased by 30 % when the flow rate was changed to 1 mL/min. A substantial reduction in the peak width and increase in noise from the peristaltic pump also accompanied with the change. Therefore the flow rate of 0.7 mL/min was selected to be the most favorable. With this condition, the maximum sampling rate was estimated to be about 36 sample/hrs.

#### 4.2.2 Operational Stability

For these experiments, the continuous injection of 200 mM glucose solution is referred to as the stability of the glucose sensor. Figure 4.13 illustrates the current response of the glucose sensor for operational stability. It was found that the percentage of relative response decreased rapidly. This can be explained by the decrease of stability due to the leaching of  $[\text{Ru}(\text{NH}_3)_6]^{3+}$  out of the films.

#### 4.2.3 Sensitivity and Calibration Curve

The conditions described previously was used for the glucose sensor. The sensitivity, linearity and response time were investigated. The sensitivity of the glucose sensor was determined by measuring of the current response at 0.7 V and 0.4 V vs. Ag/AgCl. At 0.7 V, the relationship between current response and standard glucose solution was linear as shown in figure 4.14. The sensitivity was calculated from slope (0.3 nA/mM). The slope was linear until concentration of glucose equal to 100 mM. The response time were 25 to 50 sec. The linear relationship between current response and standard glucose solution could not be obtained at 0.4 V, but the signal could be observed. It is likely that  $[\text{Ru}(\text{NH}_3)_6]^{3+}$  was leached out of the film during the measurement. Therefore, the amount of  $[\text{Ru}(\text{NH}_3)_6]^{3+}$  remaining in the film was not sufficient to transfer the electron from the redox center of the enzyme to the electrode surface.

#### 4.2.4 The Effect of Pyrrole Concentration on Glucose Response

The effect of pyrrole concentration on the current response of the glucose sensor was investigated. The electropolymerization of pyrrole was performed potentiostatically at 0.7 V vs. Ag/AgCl. The quantity of charge passed was fixed at 17 mC ( $\sim 0.3 \mu\text{m}$  thickness, assuming that  $45 \text{ mC/cm}^2$  of charge yield  $0.1 \mu\text{m}$  thickness). When the potential was applied to the cell and the small dark spot could be observed on the electrode surface and then expanded to become a continuous film. At pyrrole concentrations less than 0.1 M, the rate of oxidation of pyrrole was slow, therefore polymerization would take time. In most case the electrode surface were not completely cover with the pyrrole film. Increasing the pyrrole concentration above 0.3 M provide shorter time for polymerization, but a rugged film was formed and could be exfoliated. The resulting sensor is not sensitive to glucose solution. This can be explained that the film did not come to contact with electrode surface very well, therefore, the rate of electron transfer at the electrode surface is inhibited. The concentration of monomer in the ranges of 0.1 to 0.2 M provide the uniform film but the polymerization would take longer time.

#### 4.2.5 The Effect of $\text{Ru}(\text{NH}_3)_6\text{Cl}_3$ Concentration on Glucose Response

The effect of  $\text{Ru}(\text{NH}_3)_6\text{Cl}_3$  concentration of the glucose sensor was also investigated. As described previously in chapter III, the electrostatic binding between  $[\text{Ru}(\text{NH}_3)_6]^{3+}$  and Nafion was performed by dip-coating the Nafion electrode in  $\text{Ru}(\text{NH}_3)_6\text{Cl}_3$  solution. At concentrations less than 10 mM, the sensor did not response to glucose solution, at either 0.7 or 0.4 V vs Ag/AgCl. At concentrations above 25 mM, the electropolymerized pyrrole film did not cover the entire electrode surface. This can be explained in terms of electrostatic repulsion between  $[\text{Ru}(\text{NH}_3)_6]^{3+}$  and  $[\text{C}_4\text{H}_5\text{N}]^+$  in the electropolymerization process. Since  $[\text{Ru}(\text{NH}_3)_6]^{3+}$  is positively charged, the higher the concentration of  $[\text{Ru}(\text{NH}_3)_6]^{3+}$  in the dipping solution, the more accumulation of  $[\text{Ru}(\text{NH}_3)_6]^{3+}$  at the electrode surface. This phenomenon will inhibit the electropolymerization at the surface of the electrode. The best uniform film was obtained at 10 mM  $\text{Ru}(\text{NH}_3)_6\text{Cl}_3$ .

In this research, the method used for the electrostatic binding step provided poor reproducibility in terms of sensor fabrication. When the electrostatic binding step was finished, the Nafion/Ru electrode was left until dry. Then, it was dipped in the growth solution to perform the electropolymerization process. In this manner,  $[\text{Ru}(\text{NH}_3)_6]^{3+}$  can be leached from the electrode surface. So, the exact amount of  $[\text{Ru}(\text{NH}_3)_6]^{3+}$  can not be controlled.

#### 4.2.6 The Effect of Enzyme Concentration on Glucose Response

Since glucose oxidase is negatively charged at the neutral pH, it could presumably be incorporated into the polymer film as a counter ion of polypyrrole during electropolymerization. The amount of enzyme immobilized in the film was varied from 50 to 400 units/mL. At the concentration of 50 units/mL, the glucose sensor gave a very low response when the glucose determination was performed using flow injection system. However, the sensor fabricated under these conditions gave a signal response when the glucose determination was performed in a batch system as shown in Figure 4.15. This can be because the amount of enzyme entrapped in the film was too low. Another reason could be referred to an electronics noise from peristaltic pump. Since the signal response was in the nanoampere level, it would be sensitive to interference from the noise. At enzyme concentrations above 200 units/mL the signal response can not be observed using the flow system. This may be explained by the possibility that, because the enzyme has a high molecular weight (160,000 D), the enzyme molecules may sterically hinder the polymerization of pyrrole, resulting in polymer with shorter chain lengths. So, the enzyme can not be entrapped within the film.

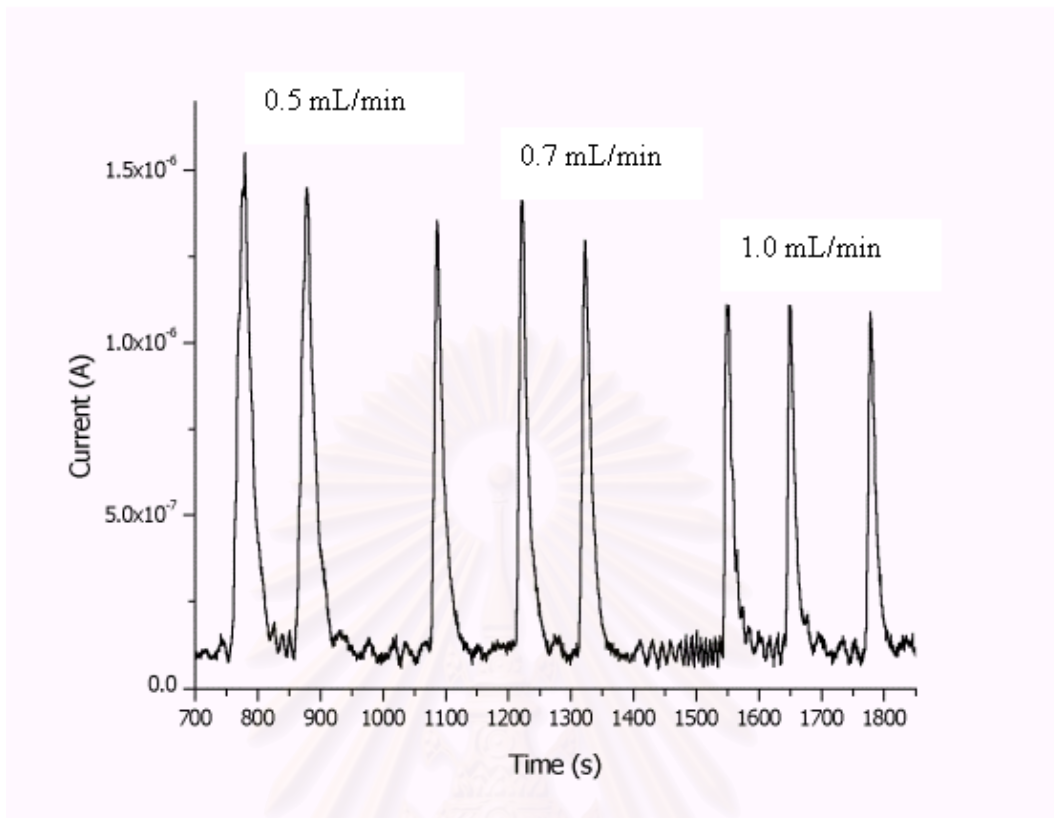


Figure 4.12 Current response to 200 mM glucose using flow injection system at 0.4 V vs Ag/AgCl. The injection volume is 100  $\mu\text{L}$ , the flow rate is 0.5, 0.7 and 1.0 mL/min, respectively

สถาบันวิทยบริการ  
จุฬาลงกรณ์มหาวิทยาลัย

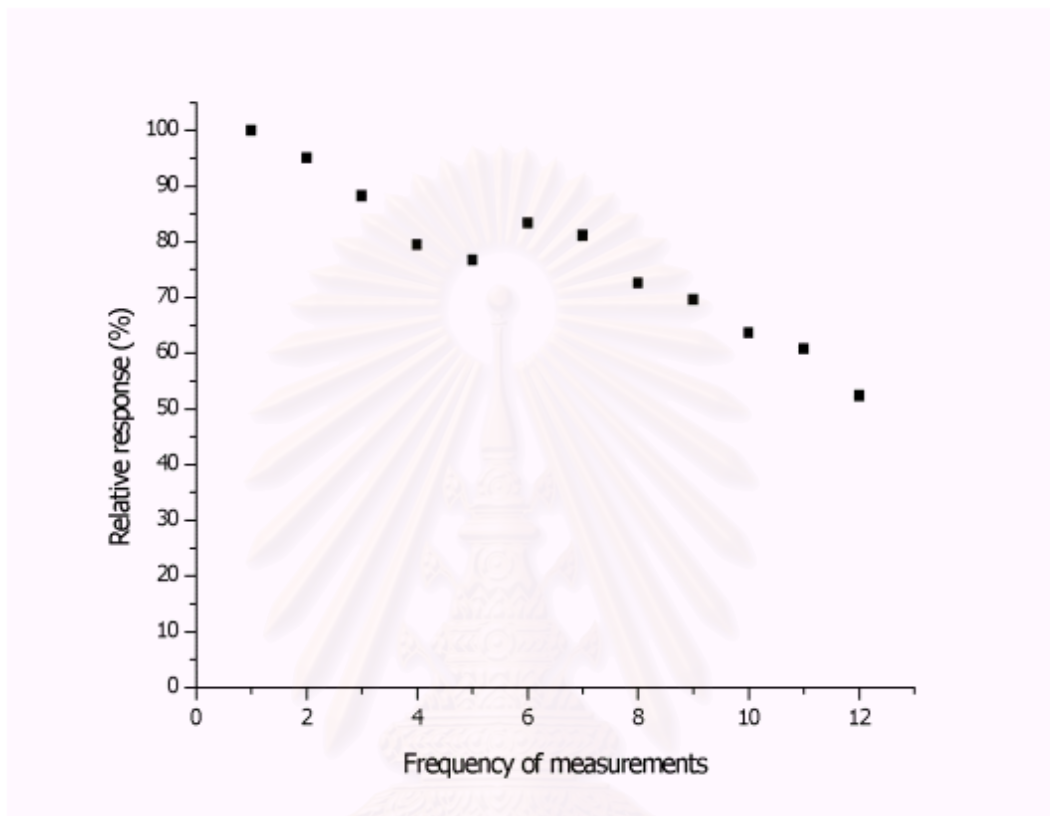


Figure 4.13 Operational stability of glucose sensor to 200 mM glucose using flow injection system at 0.4 V vs Ag/AgCl. The injection volume is 100  $\mu\text{L}$ , flow rate is 0.7 mL/min.

สถาบันวิทยบริการ  
จุฬาลงกรณ์มหาวิทยาลัย

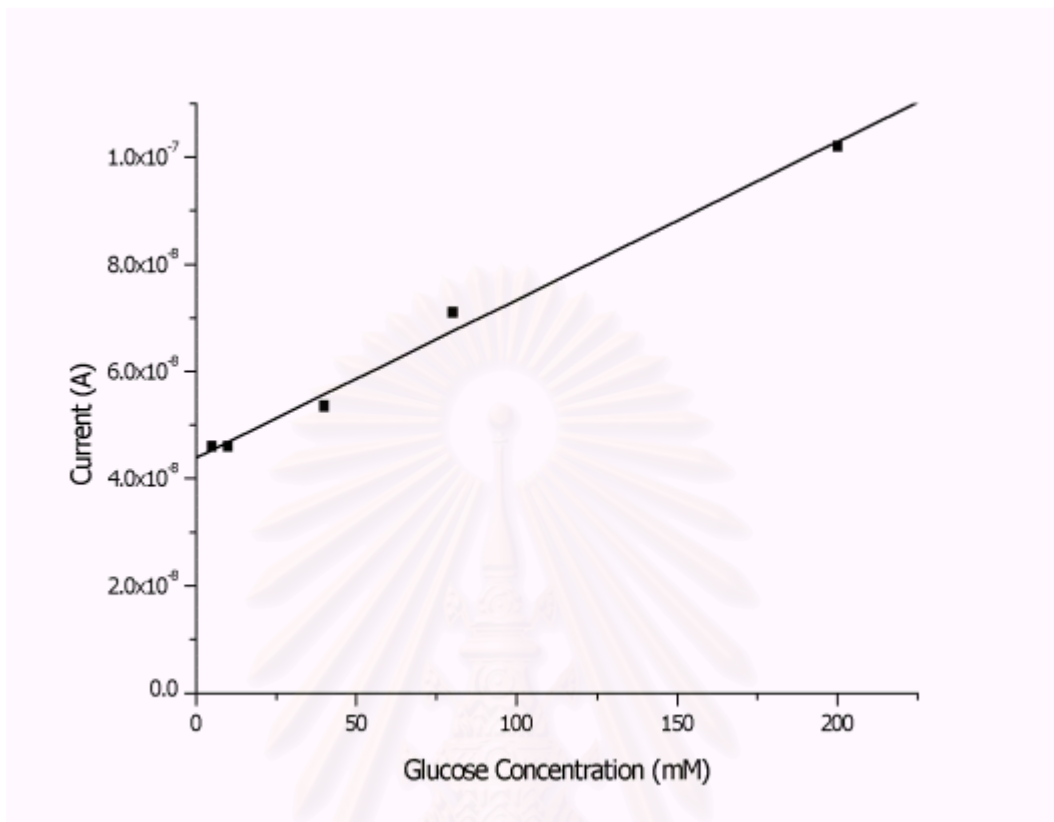


Figure 4.14 The relationship between current response and the concentration of glucose at 0.7 V vs. Ag/AgCl. The calculated slope was  $0.3 \times 10^{-9}$  ( $R^2 = 0.9916$ ).

สถาบันวิทยบริการ  
จุฬาลงกรณ์มหาวิทยาลัย

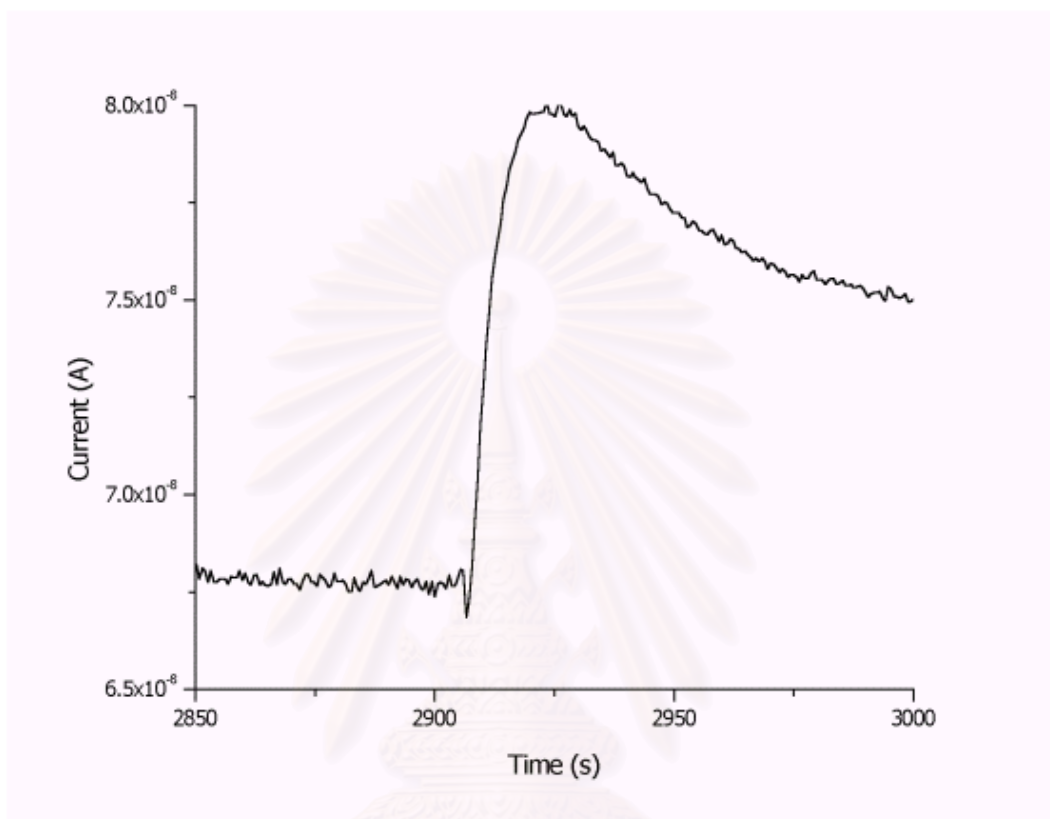


Figure 4.15 Current response to 4 mM glucose obtained from batch experiment at 0.4 V vs Ag/AgCl. The injection volume is 100  $\mu$ L.

สถาบันวิทยบริการ  
จุฬาลงกรณ์มหาวิทยาลัย



#### 4.2.7 The Effect of Film thickness on Glucose Response

The film thickness is a very important parameter for the fabrication of the sensor. The film must be thick enough to entrap the enzyme and act as a perm-selective membrane to prevent interference. However, at higher film thicknesses, it may be difficult for the substrate to reach the enzyme, leading to low signal response as well as the slow response times. In this research the film thickness was varied from 0.1 to 0.6  $\mu\text{m}$ . The thickness of the film was controlled by the amount of charge passed during electropolymerization and estimated by assuming that 45  $\text{mC}/\text{cm}^2$  of charge yields a 0.1  $\mu\text{m}$  thick film. At 5.56  $\text{mC}$  ( $\sim 0.1 \mu\text{m}$ ), the film did not cover the entire surface of the electrode. It can be presumed that the assumption described above depends on the efficiency of the polymerization reaction and the surface conditions of the electrode (in this research, the electrode was pre-coated with Nafion). Uniform films were observed when over 17  $\text{mC}$  ( $\sim 0.3 \mu\text{m}$ ) of charge were passed.

#### **Procedure II**

Determination of glucose in flow experiment was performed using *flow cell III*. Figure 4.17 and 4.18 show the relationship between current response and the concentration of glucose at 0.7V vs. Ag/AgCl. The conditions were shown in Table 4.4 and Table 4.5. The electropolymerization of pyrrole in KCl solution provided shorter polymerization time; therefore, the thick film can be prepared. Moreover, the sensor fabricated by this procedure gave the better sensitivity.

**Table 4.4** The conditions for the preparation of glucose sensor (procedure II).

Volume of Nafion in the pre-coating step:	2 $\mu\text{L}$
Growth solution:	
0.1 M KCl	
Total volume 5 mL containing	
Pyrrole	0.1 M
glucose oxidase	100 Units/mL
Ru(NH <sub>3</sub> ) <sub>6</sub> Cl <sub>3</sub>	5 mM
Polymerization potential:	Potentiostatic at 0.7 V
(Pre-adsorption of [Ru(NH <sub>3</sub> ) <sub>6</sub> ] <sup>3+</sup> for 10 min at 0.0 V)	
Charge:	40 mC (0.7 $\mu\text{m}$ thickness)

**Table 4.5** The conditions for flow injection system (procedure II).

Flow system:	Single line mode
Flow cell configuration:	<i>Flow cell III</i>
Operating potential for determination of glucose:	0.7 and 0.4V vs. Ag/AgCl
Carrier stream:	0.1 M phosphate buffer solution, pH 7.0
Flow rate:	0.7 mL/min
Injection volume of sample:	100 $\mu\text{L}$

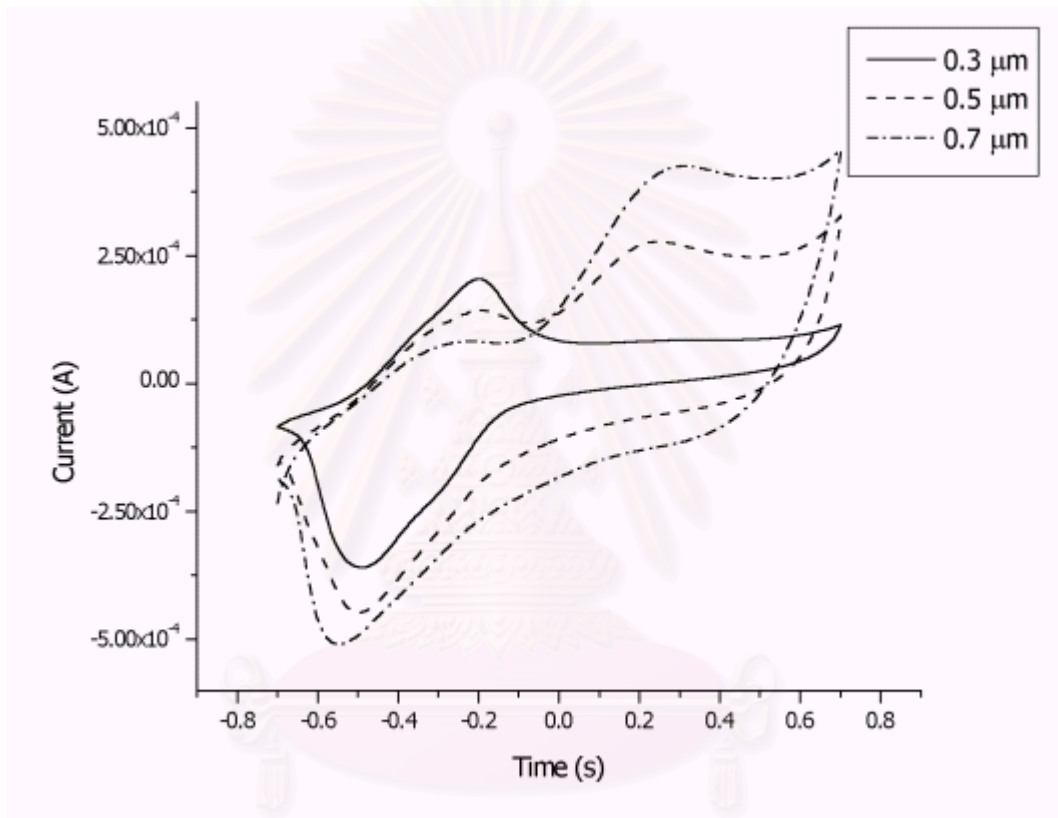


Figure 4.16 Cyclic voltammograms in 0.1 M phosphate buffer solution from -0.7 to 0.7 V vs. Ag/AgCl, scan rate 0.1 V/sec obtained from the glucose sensor at different film thickness. Counter electrode was platinum.

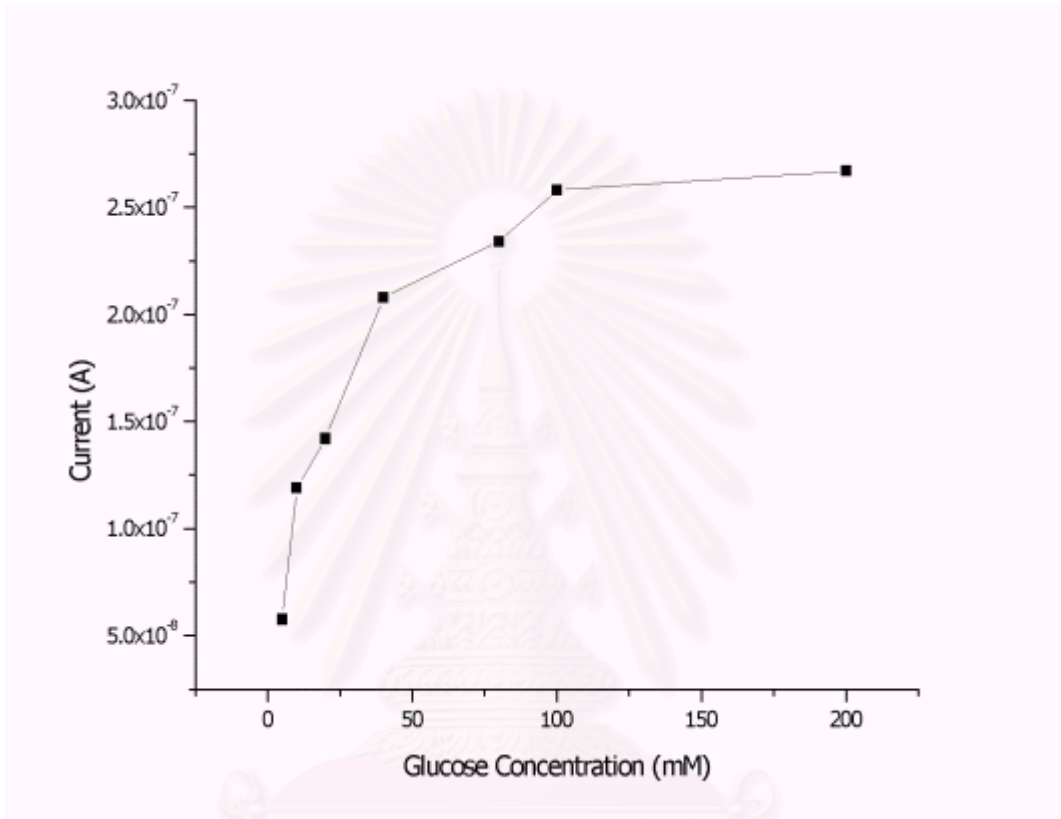


Figure 4.17 The relationship between current response and the concentration of glucose at 0.7 V vs. Ag/AgCl. (the sensor was fabricated from procedure II)

สถาบันวิทยบริการ  
จุฬาลงกรณ์มหาวิทยาลัย

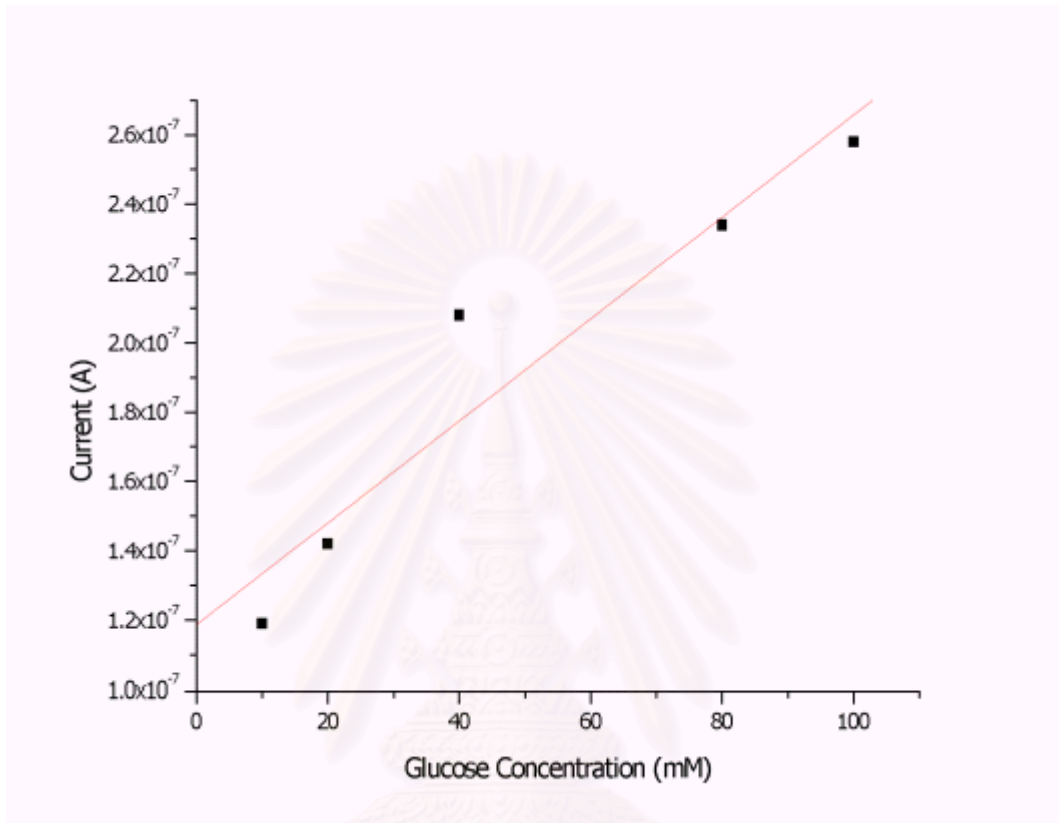


Figure 4.18 The relationship between current response and the concentration of glucose at 0.7 V vs. Ag/AgCl. The calculated slope was  $1.47 \times 10^{-9}$  ( $R^2 = 0.9554$ ). The sensor was fabricated from procedure II.

สถาบันวิทยบริการ  
จุฬาลงกรณ์มหาวิทยาลัย

### 4.3 Interference Studies

The determination for interferences such as ascorbic acid and acetaminophen are referred to selectivity of the sensor. The interferences from these two species always observed with amperometric sensor due to oxidation at a high operating potential. The Table 4.6 shows the current from ascorbic acid and acetaminophen using the optimized glucose sensor at 0.7 V vs. Ag/AgCl. It was found that the glucose sensor could prevent the oxidation of compounds. The current response to 2 mM acetaminophen can not be observed. The interfering from 2 mM ascorbic acid can be minimized more than 99 %.

**Table 4.6.** The current measurement of interferences at 0.7 V

Analyte	Current (A)
20 mM Glucose	$1.42 \times 10^{-7}$
5 mM Glucose	$5.77 \times 10^{-8}$
2 mM Ascorbic acid	$3.85 \times 10^{-8}$
2 mM Acetaminophen	none

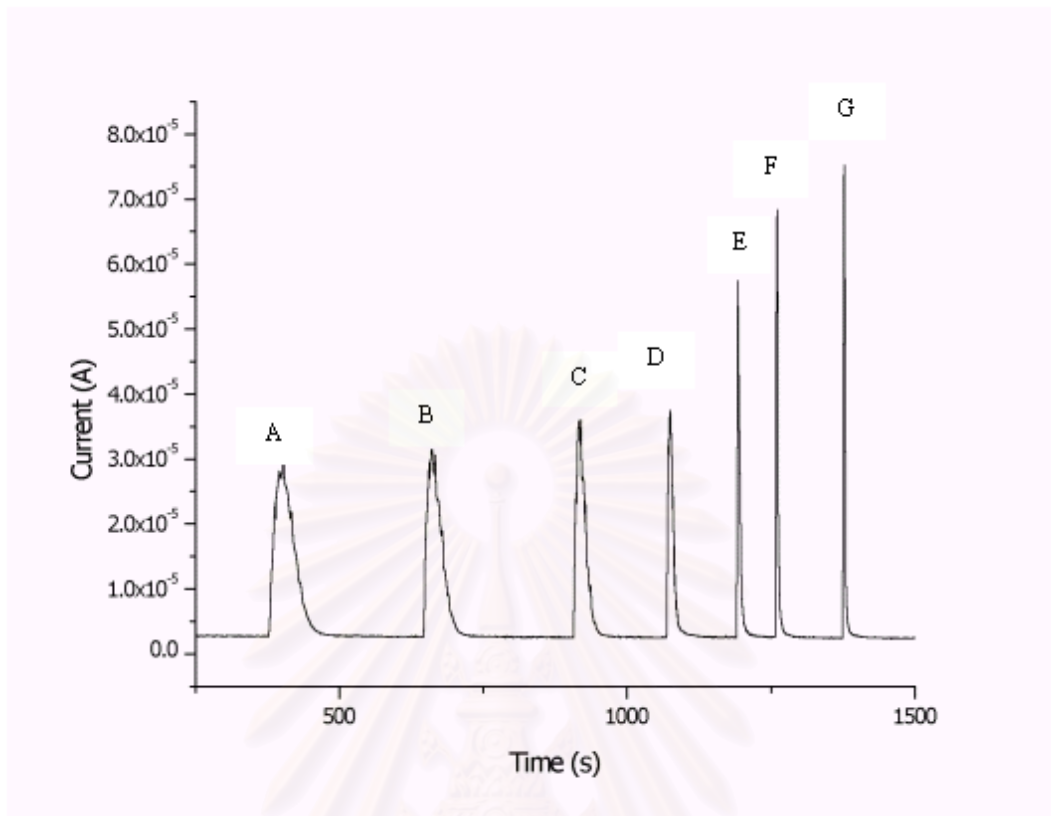


Figure 4.19 Current response to 2 mM ascorbic acid using flow injection system at 0.7 V vs Ag/AgCl. The injection volume is 100  $\mu\text{L}$ . (A, B, C, D, E, F, and G represent the flow rate of 0.5, 0.7, 1.0, 2.0, 3.0, 4.0 and 5.0 mL/min, respectively)

สถาบันวิทยบริการ  
จุฬาลงกรณ์มหาวิทยาลัย

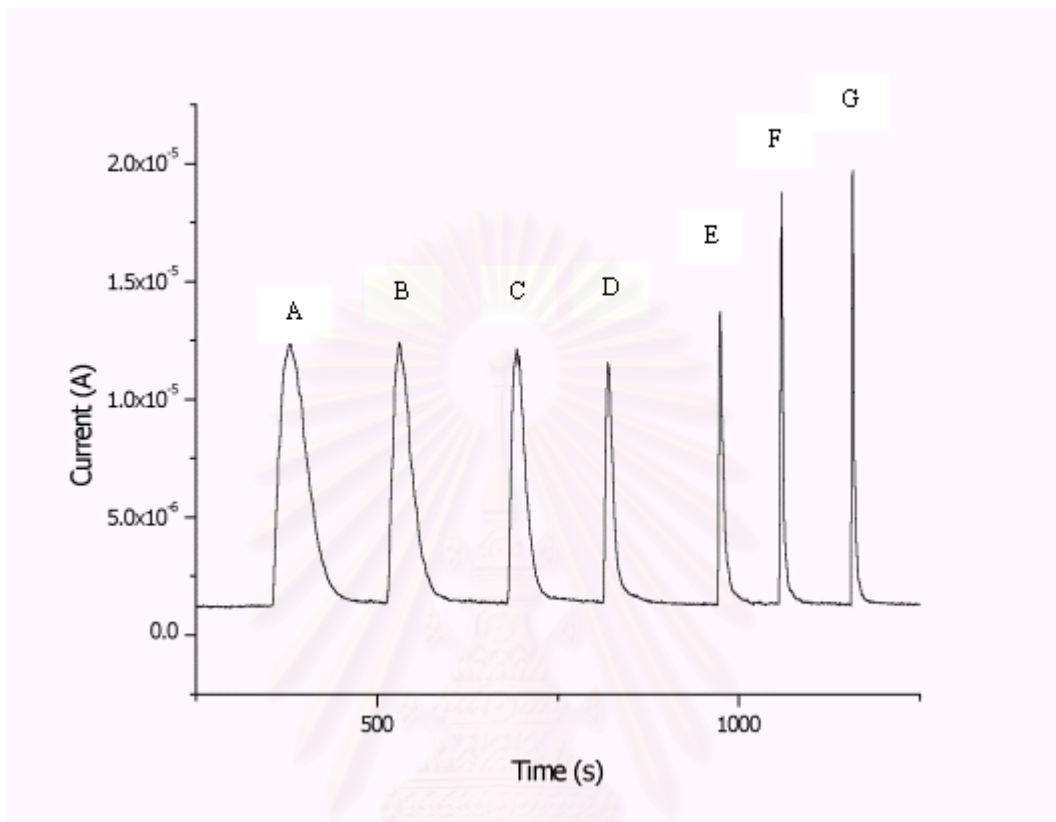


Figure 4.20 Current response to 2 mM ascorbic acid using flow injection system at 0.4 V vs Ag/AgCl. The injection volume is 100  $\mu$ L. (A, B, C, D, E, F, and G represent the flow rate of 0.5, 0.7, 1.0, 2.0, 3.0, 4.0 and 5.0 mL/min, respectively)

สถาบันวิทยบริการ  
จุฬาลงกรณ์มหาวิทยาลัย



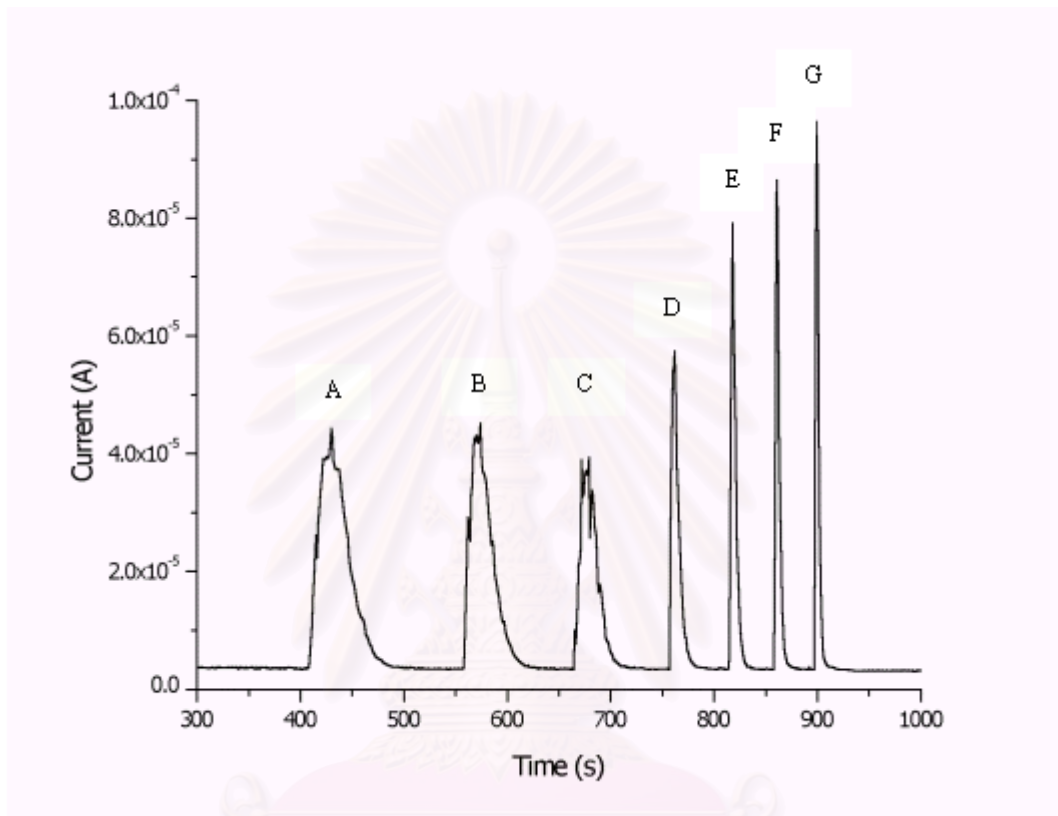


Figure 4.21 Current response to 2 mM acetaminophen using flow injection system at 0.7 V vs Ag/AgCl. The injection volume is 100  $\mu$ L. (A, B, C, D, E, F, and G represent the flow rate of 0.5, 0.7, 1.0, 2.0, 3.0, 4.0 and 5.0 mL/min, respectively)

สถาบันวิทยบริการ  
จุฬาลงกรณ์มหาวิทยาลัย

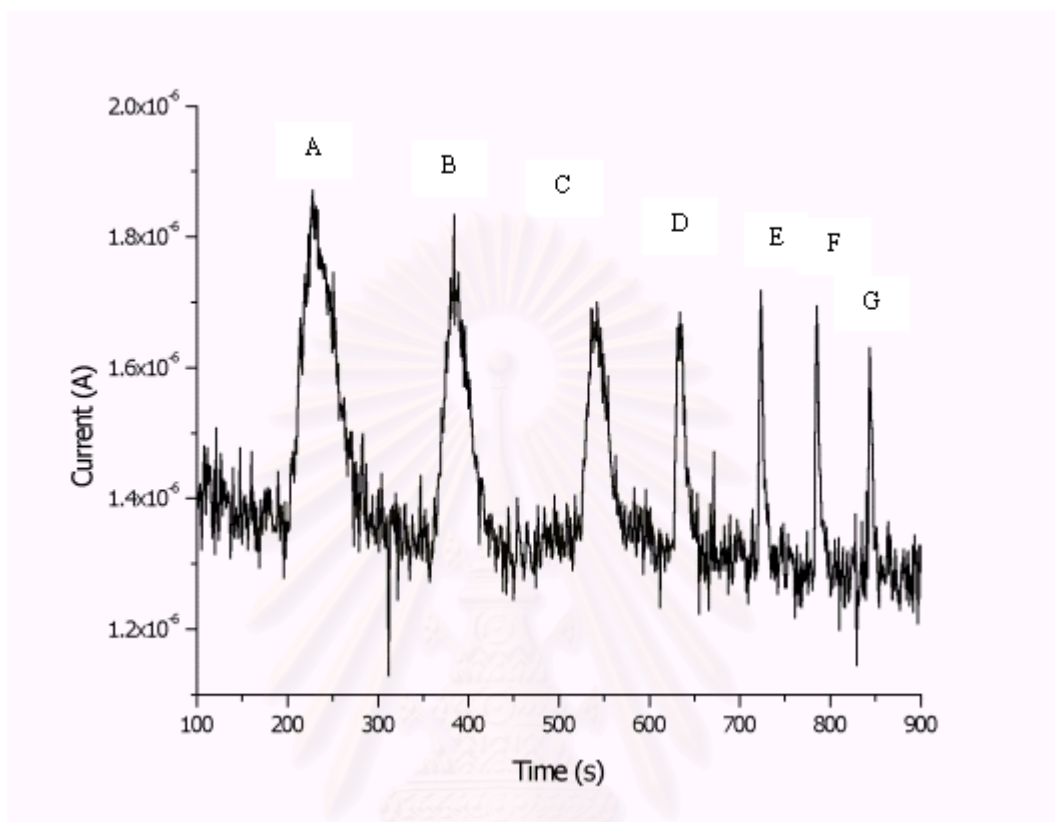


Figure 4.22 Current response to 2 mM acetaminophen using flow injection system at 0.4 V vs Ag/AgCl. The injection volume is 100  $\mu\text{L}$ . (A, B, C, D, E, F, and G represent the flow rate of 0.5, 0.7, 1.0, 2.0, 3.0, 4.0 and 5.0 mL/min, respectively)

สถาบันวิทยบริการ  
จุฬาลงกรณ์มหาวิทยาลัย

## CHAPTER V

### CONCLUSION

An amperometric glucose sensor was fabricated by the electrochemical polymerization of polypyrrole onto a gold electrode, pre-coated with Nafion, in the presence of the enzyme glucose oxidase and  $[\text{Ru}(\text{NH}_3)_6]^{3+}$  at a potential of 0.7 V vs. Ag/AgCl. The enzyme and  $[\text{Ru}(\text{NH}_3)_6]^{3+}$  were entrapped onto the films during the polymerization process. The electrodes with surface area of  $0.1257 \text{ cm}^2$  were used for the preparation of the sensor. Glucose response was determined by the measurement of the amperometric oxidation of  $[\text{Ru}(\text{NH}_3)_6]^{3+}$  at 0.7 V and 0.4 V vs. Ag/AgCl using a flow injection system. The sensitivity of the glucose sensor operated at 0.7 V vs. Ag/AgCl was  $1.47 \text{ nA/mM}$ . The optimized sensor can be operated at 0.7 V with a low level of interference. The current response to glucose at 0.4 V can be observed, but cannot be used for quantitative analysis. The modified sensor can be operated at 0.4 V for only a few assays, because the  $[\text{Ru}(\text{NH}_3)_6]^{3+}$  leached out during glucose measurement. Therefore,  $[\text{Ru}(\text{NH}_3)_6]^{3+}$  may be regarded as an inappropriate mediator for the flowing system. New preparation procedures are required in order to improve the stability of the sensor. The application of the glucose sensor using  $[\text{Ru}(\text{NH}_3)_6]^{3+}$  as an electron mediator for glucose determination at 0.4 V using a flow-injection system is less advantageous. However, it is favorable when considering the simplicity of renewal and the possibility of modification of the sensor.

## SUGGESTIONS FOR FURTHER WORK

1. The preparation procedure of the sensor in this research has too many steps. Therefore, the error may occur what could not be controlled. New preparation procedures with fewer steps are required. The electrostatic binding step and electropolymerization step can be proceeded in a single step by mixing of  $\text{Ru}(\text{NH}_3)_6\text{Cl}_3$  in the growth solution.

2. An enzyme immobilization method such as covalent bonding and cross-linking could be the appropriate method for the flow injection system. The direct bonding between enzyme and the matrices may be lead to better stability of the sensor.

3. Determination of glucose in real samples and interference studies should be investigated.

4. Attaching the electron mediator directly with flexible spacers to the enzyme as well as wiring the enzyme (covalently binding mediator with enzyme) may be lead to better contact with the electrode surface and better stability of the sensor.

5. A conducting polymer such as poly(*N*-methyl pyrrole) or polyphenol could be used as new polymeric matrices for enzyme immobilization. The physical properties of electropolymerized films, such as porosity, must be studied.

6. Metal-porphyrin complex, such as cobalt-porphyrin and ruthenium-porphyrin can be used as electron mediators. Because porphyrin can be derived from pyrrole and have the same basic structure, therefore, they could be incorporated in the polymeric frame work of polypyrrole or poly(*N*-methyl pyrrole) with a high compatibility.

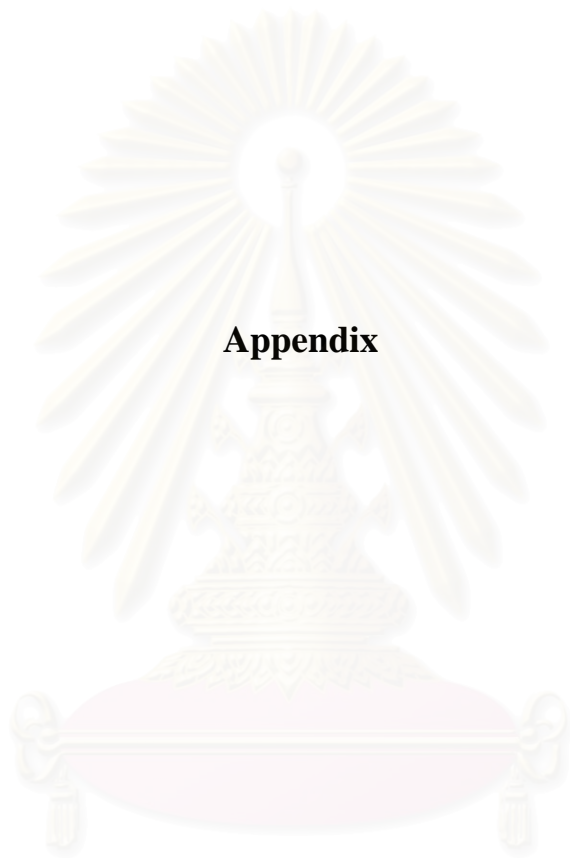
## REFERENCES

- (1) Turner, A. P. F.; Karube, I.; and Wilson, G. S. *Biosensors: Fundamentals and Applications*; Oxford University Press: Oxford, 1987.
- (2) Mosbach, K. *Immobilized Enzymes and Cells: Part D*; Academic Press: San Diego, 1988.
- (3) Du, G.; Lin, C.; and Bocarsly, A. B. *Anal. Chem.* **1996**, *68*, 796-806.
- (4) Bartlett, P. N.; Ali, Z.; and Eastwick-field, V. Electrochemical immobilisation of enzymes: Part 4. - Co – immobilisation of glucose oxidase and ferro/ferricyanide in poly(N-methylpyrrole) films. *J. Chem. Soc. Faraday Trans.* **1992**, *88*, 2677-2683.
- (5) Foulds, N. C.; and Lowe, C. R. Immobilization of glucose oxidase in ferrocene-modified pyrrole polymers. *Anal. Chem.* **1988**, *60*, 2473-2478.
- (6) Gros, P.; and Bergel, A. Improved model of a polypyrrole glucose oxidase modified electrode. *J. Electroanal. Chem.* **1995**, *386*, 65-73.
- (7) Fortier, G.; Brassard, E.; and Belanger, D. Optimization of a polypyrrole glucose oxidase biosensor. *Biosensor & Bioelectronics* **1990**, *5*, 473-490.
- (8) Imisides, M.D.; Jonh, R.; and Wallace, G. G. Microsensors based on conducting polymers. *CHEMTECH* **1996**, *26*, 19-25.
- (9) Trojawicz, M.; Matuszewski, W.; and Podsiadia, M. Enzyme entrapped polypyrrole modified electrode for flow-injection determination of glucose. *Biosensors & Bioelectronics* **1990**, *5*, 149-156.
- (10) Turner, A. P. F.; Morris, N. A.; Cardosi, M. F.; and Birch, B. J. An electrochemical capillary fill device for the analysis of glucose incorporating glucose oxidase and ruthenium (III) hexamine as mediator. *Electroanalysis* **1992**, *4*, 1-9.
- (11) Bartlett, P. N.; and Caruana, D. J. Electrochemical immobilization of enzymes: Part V. Microelectrodes for the detection of glucose based on glucose oxidase Immobilized in a poly (phenol) film. *Analyst* **1992**, *117*, 1287-1292.
- (12) van Os, P. J. H. J.; Bult, A.; and van Bennekom, W. P. A glucose sensor, interference free for ascorbic acid. *Analytica Chimica Acta* **1995**, *305*, 18-25.
- (13) Pei, J.; and Li, X. Amperometric glucose enzyme sensor prepared by immobilizing glucose oxidase on CuPtCl<sub>2</sub> chemically modified electrode. *Electroanalysis* **1999**, *11*, 1266-1272.

- (14) Rivas, G. A.; and Rodriquez, M. C. Glucose sensor prepared by the deposition of iridium and glucose oxidase on glassy carbon transducer. *Electroanalysis* **1999**, *11*, 558-564.
- (15) Ataai, M. M.; Beckman, E. J.; and Almeida, N. F. **Immobilization of glucose oxidase in thin polypyrrole films : Influence of polymerization conditions and film thickness on the activity and stability of the immobilized enzyme**. *Biotechnology and Bioengineering* **1993**, *42*, 1037-1045.
- (16) Cunningham, A. J. *Introduction to Bioanalytical Sensors*; Wiley: New York, 1998.
- (17) Wang, J. *Analytical Electrochemistry*; Wiley-VCH: New York, 1994.
- (18) Bard, A. J.; and Faulkner, L. R. *Electrochemical Methods: Fundamentals and Applications*; Wiley: New York, 1980.
- (19) Ruzicka, J.; and Hansen, E. H. *Flow-Injection Analysis*, 2 ed.; Wiley: New York, 1988.



สถาบันวิทยบริการ  
จุฬาลงกรณ์มหาวิทยาลัย



**Appendix**

สถาบันวิทยบริการ  
จุฬาลงกรณ์มหาวิทยาลัย

## APPENDIX A

### ASSEMBLY OF DISK ELECTRODE

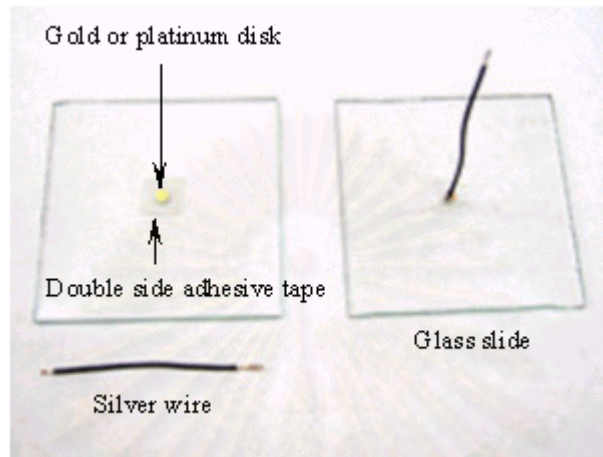


Figure A1. Gold or platinum disk with 4 mm in diameter and silver wire.

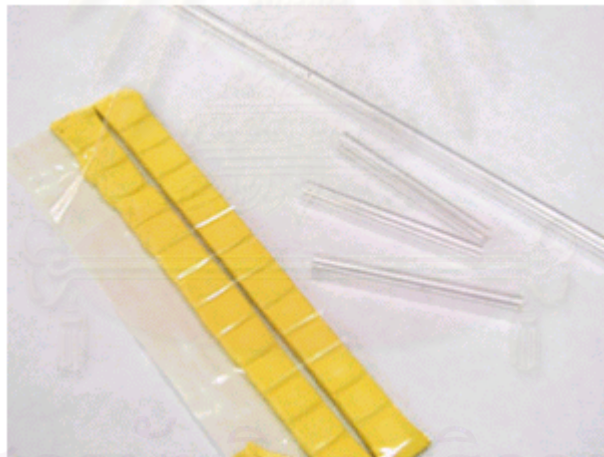
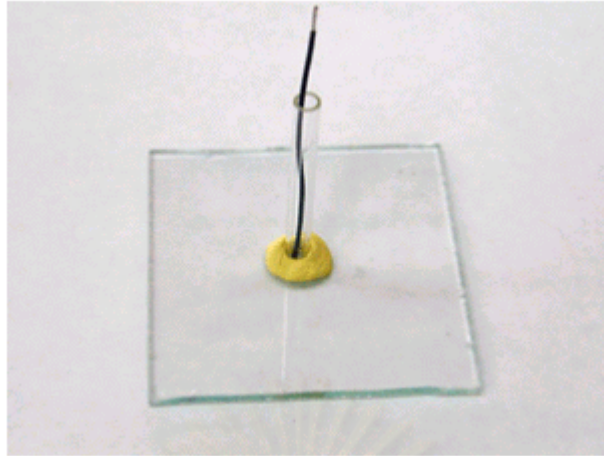
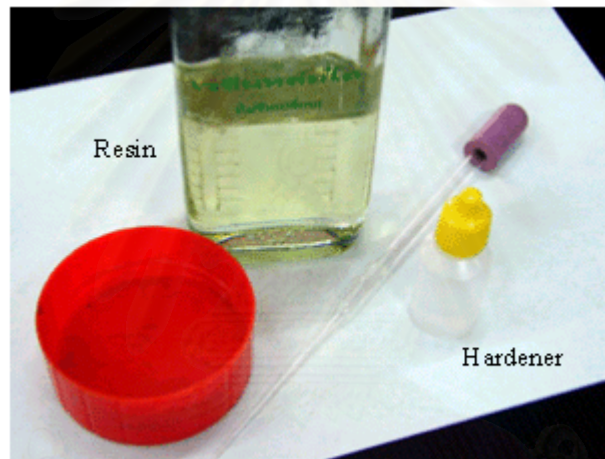


Figure A2. Glass tube with 4 mm in inner diameter and pate adhesive.





**Figure A3. Glass tube was adhered to the glass slide with pate adhesive.**



**Figure A4. Polymer resin and hardener.**

สถาบันวิทยบริการ  
จุฬาลงกรณ์มหาวิทยาลัย

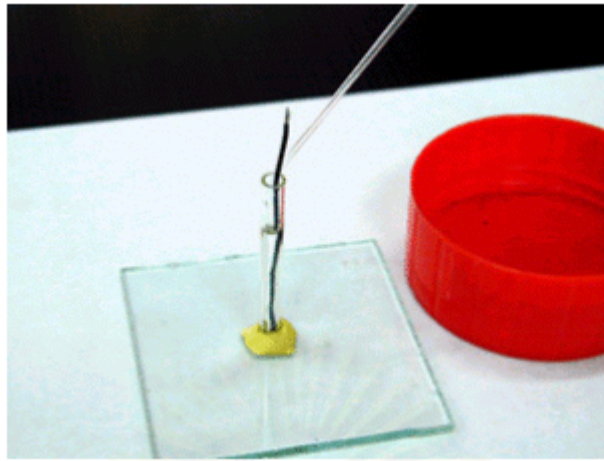


**Figure A5. The glass tube with mixture of resin and hardener.**

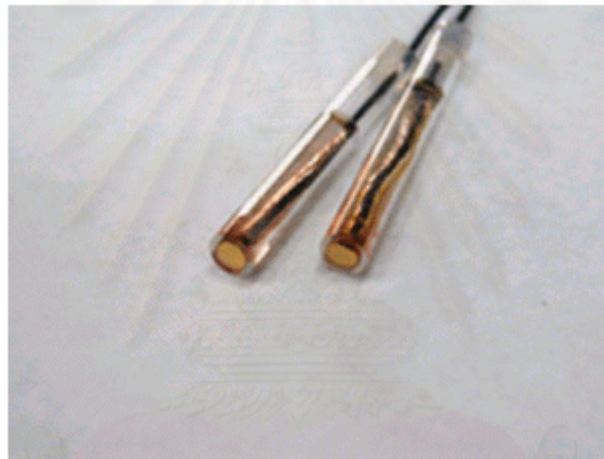


**Figure A6. The finished disk electrodes.**

สถาบันวิทยบริการ  
จุฬาลงกรณ์มหาวิทยาลัย

## APPENDIX B

### Electropolymerization of Polypyrrole

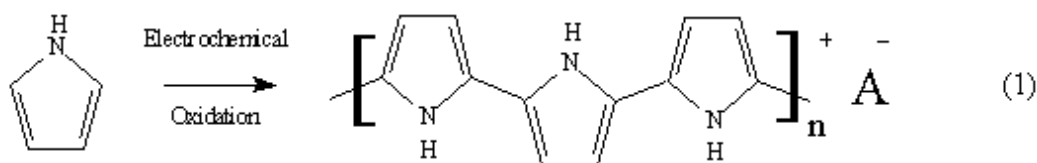
#### Introduction to Conducting Polymers

Conducting polymers are polymeric materials containing extended conjugated  $\pi$ -electron backbones. They display unusual electronic properties, such as low energy optical transition, low ionization potentials and high affinities. Such polymers are easily oxidized or reduced by charge-transfer agents (*dopants*) that act as electron acceptors or electron donors, respectively. This results in a class of polymers that can be oxidized or reduced more reversibly than conventional polymers. These materials may be prepared by electrochemically, typically by oxidizing of their monomers in the presence of an electrolyte in aqueous or organic solutions. Passage of current through this solution result in the loss of electrons, and compounds are oxidized at the anode. Electrons are gained and compounds are reduced at the cathode. This process is referred to an electrochemical polymerization when polymer is formed.

Charge transfer agents affect this oxidation or reduction by entering or leaving the film as the oxidation state changes. This process can convert the insulating polymers to conducting polymers. During the polymer synthesis, the incorporation of extended  $\pi$ -electron conjugation is importance. The monomeric materials therefore typically contain aromatic or multiple carbon-carbon bonds, that must be preserved in the polymer backbone. Interesting conducting polymers include polypyrrole, polyaniline and polythiophene.

สถาบันวิทยบริการ  
จุฬาลงกรณ์มหาวิทยาลัย

It is generally accepted that the electrochemical polymerization of heterocyclic monomers is came out as follow:



The mechanism for polymerization (Figure B1) involves oxidation of pyrrole at the  $\alpha$ -position to form a radical-cation (**I**), which undergoes radical coupling to yield the dimer-dication (**II**). The latter loses two protons to yield the dimer (**III**). The dimer repeats to form a dimer radical-cation, coupling with itself and **I** to form the tetramer-dication and trimer-dication, respectively, followed by losing two protons to yield tetramer and trimer. Propagation of polymer is proceeded via repetition of the same sequence-one electron loss, coupling of different-sized radical-cations, deprotonation. Electrochemical polymerization, as usually carried out, does not yield the neutral form. One cycle back and forth between the conducting form and nonconducting form, coloured black and light yellow, respectively, by reversing polarity. The doped polymer would have a structure such as **IV**, where  $A^-$  is the anion of the electrolyte. The doped polymer precipitates out and coats the surface of the anode during polymerization. The polymerization reaction and polymer properties (conductivity and mechanical strength) are dependent on such parameters as identity and concentration of electrolyte, reaction temperature, and current density. The dimerization rate increased as the square of the radical cation concentration increased, leading to a much greater consumption of this species as the rate of pyrrole oxidation and the active electrode area increased with pyrrole concentration.

สถาบันวิทยบริการ  
จุฬาลงกรณ์มหาวิทยาลัย

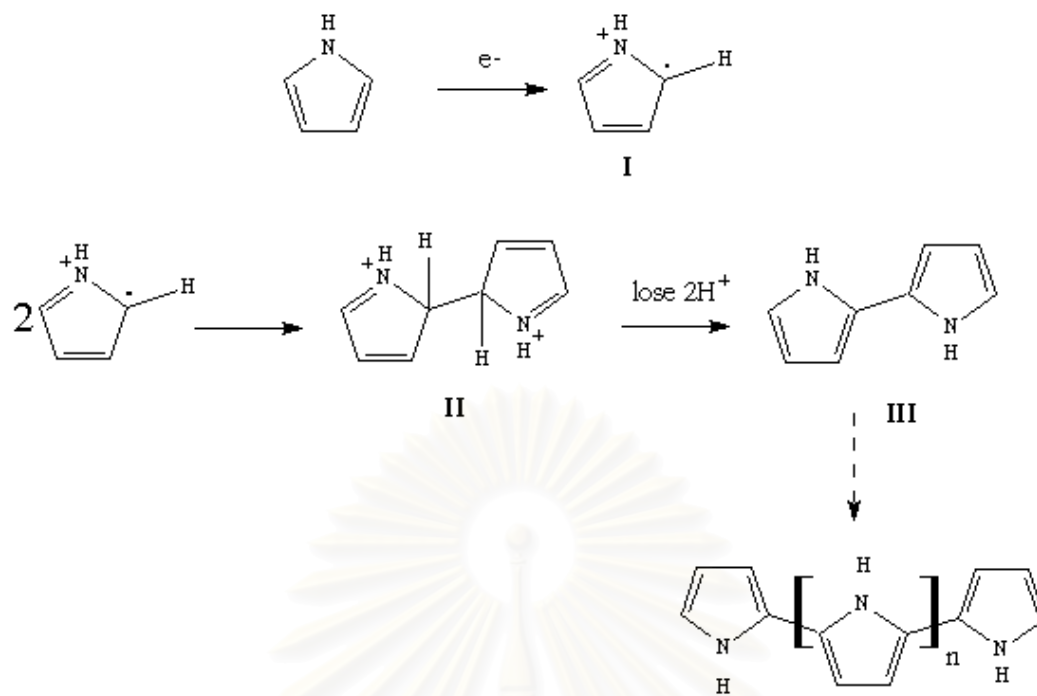


**Figure B1.** Mechanism of pyrrole polymerization

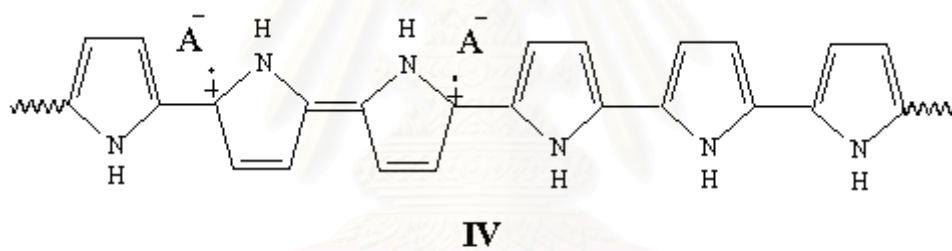


**Figure B2.** Structure of the doped polypyrrole

สถาบันวิทยบริการ  
จุฬาลงกรณ์มหาวิทยาลัย

## Permselective Film Conducting Polymers for Enzyme Electrode

Permselective films greatly enhance the selectivity and stability of amperometric probes by rejecting interference from the electrode surface. The processing of polypyrrole highlights the utility and the limitations of most conducting polymers as far as biosensors are concerned. Polypyrrole can be electrochemically polymerized from aqueous media at neutral pH, which allows the incorporation of a wide range of counter ions. Other conducting polymers are more limited in this regard.

Polymer modified electrodes have been received extensive interest since they can be designed to provide important improvements in stability and selectivity. Selectivity of polymer modified electrodes can be attained by different mechanisms such as size exclusion, ion exchange, and hydrophobic interactions. Polymer modified electrodes obtained from the electrochemical polymerization of pyrrole have received great attention in view of several promising applications including the development of chemical and biochemical sensors.

The entrapment of enzymes within electrochemical polymerized film offers the possibility of attaching the biocatalysts to conducting surfaces. Electrochemical polymerization of polypyrrole proceeds via highly reactive  $\pi$ -radical cations which react with other pyrrole molecules to form chains with mainly  $\alpha,\alpha'$ -coupling. Since the polymer is positively charged, anions from the solution are accumulated in the film. The negative charge of enzyme oxidase at pH 7.0 decisively influences the positively charged matrix and polymer-enzyme stabilization occurs from the electrostatic interaction between the positively charged polymer and the negatively charged enzyme. In addition, the porosity of the films is generally controlled by the counter ions.

## VITA

Mr. Passapol Ngamukot was born on October 16, 1975 at Chulalongkorn Hospital, Bangkok. He received a Bachelor Degree of Science in Chemistry from Faculty of Science, Chulalongkorn University in 1998. After that, he started to study in Graduate School, Chulalongkorn University for the Master Degree of Science. He has been a graduate student, study in Analytical Chemistry in Chulalongkorn University.



สถาบันวิทยบริการ  
จุฬาลงกรณ์มหาวิทยาลัย